Fidelity of Flight Control Systems in a Real-Time Optimal Trajectory Planner

by

Toni El-Dirani

B.S., Massachusetts Institute of Technology (1990)

Submitted to the Department of Aeronautics and Astronautics
in partial fulfillment of the requirements for the degree of

Master of Science in Aeronautics and Astronautics

at the

MASSACHUSETTS INSTITUTE OF TECHNOLOGY

June 1991

Author . . . .
Department of Aeronautics and Astronautics
March, 7 1991

Certified by . . . .
Wallace E. Vander Velde
Professor
Thesis Supervisor

Accepted by . . . .
Prof. Harold Wachman
Chairman, Department Graduate Committee
Aero

Fidelity of Flight Control Systems in a Real-Time Optimal Trajectory Planner

by

Toni El-Dirani

Abstract

An integral part of a Mission Planning System consists of an algorithm to optimize the trajectory of a fighter aircraft. Such an optimization accounts for potential threats and their geographic locations en route. In the past, different algorithms were devised to optimize a pre-selected performance measure leading to an optimal trajectory. However, the algorithms used a simplified model of the aircraft dynamics and its flight control systems.

The objective of this research is to investigate the required fidelity of the models of the aircraft's flight control systems used in the trajectory planning process. A simulation depicting the full dynamics of the aircraft was performed. Two flight control systems were designed and their responses to deterministic disturbance models of wind gusts and wind shears were evaluated. In addition, a stochastic analysis of the flight control systems was performed and their minimum degree of complexity in the optimizing algorithm was determined.

Thesis Supervisor: Wallace E. Vander Velde
Title: Professor

Acknowledgments

A sincere note of gratitude goes to Professor W. Vander Velde for his great support and insightful comments during the progress of this research. The experience gained from working with him is deeply appreciated.

Also I would like to thank all the members of my family for their encouragement and invaluable support. I am indebted to them for everything I have achieved and am very thankful to have them as a family.

Contents

Nomenclature

a_{Nc}	Normal acceleration command (ft/sec^2)
$\tilde{a}_N$	Normal acceleration command update (ft/sec^2)
G_{lat}	Lateral feedback gain matrix
G_{long}	Longitudinal feedback gain matrix
$L_i(i = u, v, w)$	Wind gust scale lengths (ft)
p_g	Roll due to gradient of w_g along the span of the aircraft $(1/sec)$
p	Perturbed roll rate (deg/sec)
P	State covariance matrix
(Q, R)	LQR penalty matrices
S	Sensitivity function
q	Perturbed pitch rate (deg/sec)
r	Perturbed yaw rate (deg/sec)
(u, v, w)	Perturbed components of the aircraft velocity (ft/sec)
(u_g, v_g, w_g)	Wind velocity components (ft/sec)
U_0	Nominal aircraft forward velocity (ft/sec)
V_m	Maximum wind velocity (ft/sec)
$\underline{w}(t)$	Gaussian white noise vector
(x, y, z)	Inertial coordinates of the aircraft position
(X, Y, Z)	Aircraft stability axes system
α	Perturbed angle of attack (deg)
δ_a	Aileron deflection (deg)
δ_e	Elevator deflection (deg)
δ_r	Rudder deflection (deg)
δ_T	Throttle angle (deg)
ϕ_c	Roll angle command (deg)
$\tilde{\phi}$	Roll angle command update (deg)
ϕ	Perturbed roll angle (deg)
Φ_0	Nominal aircraft roll angle (deg)

$\Phi_i(i = u, v, w)$	Dryden gust spectra of air turbulence
θ	Perturbed pitch angle *(deg)*
Θ_0	Nominal aircraft pitch angle *(deg)*
Ω	Spatial frequency of air turbulence waves *(rad/ft)*
ψ	Perturbed yaw angle *(deg)*
Ψ_0	Nominal aircraft roll angle *(deg)*
σ_0	Frequency of non-minimum phase zero *(rad/sec)*
$\bar{\sigma}$	Maximum singular value
$\sigma_i(i = u, v, w)$	Gust intensities associated with u_g, v_g, w_g *(ft/sec)*

List of Figures

Chapter 1

Introduction

1.1   Concept of Optimal Trajectory Planner

As the objectives of a fighter aircraft mission increase, so does the pilot workload. In addition to the regular navigational tasks, the pilot would be responsible for meeting various mission requirements. He would have to insure the success of the mission by avoiding possible ground threats en route. The geographic locations of radars have a principal impact upon planning a "safe" flight path. Moreover, the pilot would be required to meet time and fuel constraints simultaneously. Such constraints are imposed by the aircraft's fuel consumption and the possibility of mobile ground targets. Other conceivable obstacles to overcome during the mission are natural threats like weather conditions and terrain nature.

Severe thunderstorms may jeopardize the feasibility of a mission and its success. They can cause significant changes in planning a minimum risk flight path and, consequently, a possible exposition of the aircraft to radars or missile sites.

In general, mountain terrain demands substantially rapid maneuvering. The aircraft's structural limits can be reached while following a steeply varying terrain. Furthermore, the pilot's ability to maneuver may deteriorate trying to avoid nearby ground threats. In order to alleviate the pilot workload, the concept of an automatic mission planning system was devised.

For the purpose of this research, the mission planning system can be thought to con-
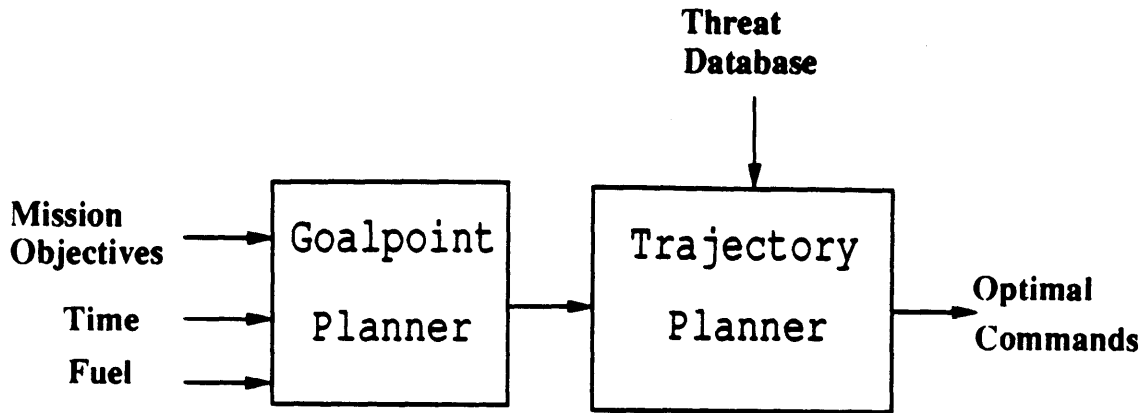
Figure 1-1: Mission Planning System

sist of a goal point planner and a trajectory planner (figure 1-1). General mission objectives along with time and fuel constraints form the input to the goal point planner. The output of the goal point planner is a set of waypoints whose separation is about 5000 meters. Each waypoint is characterized by a neighborhood through which the optimal trajectory must pass. Trajectory segments are planned to encompass several waypoints ahead. The strategy is to fly the trajectory segment leading to the first waypoint. As this waypoint is passed, a new trajectory segment is planned to capture the second waypoint. Each trajectory segment is constrained to begin with the actual position and velocity of the aircraft. In this context, a discrete time feedback of position and velocity information is present. It remains to investigate whether the effect of air turbulence is significant enough to require continuous position and velocity feedbacks between the waypoints.

A database depicting potential threats and their geographic locations is made available. The trajectory planner performs an optimization on a "risk" function and produces the corresponding optimal flight commands. In this thesis, it is assumed that the commands generated by the planner are suitable inputs for the aircraft's flight control systems [2]. Once applied, these commands give rise to a flight path that minimizes the effects of the threats according to their gravity.

1.2 Thesis Objectives

Models of the flight control systems must be embedded in the optimization process. In previous works [1, 2], simple models of the flight control systems were used in different optimizing algorithms to generate suitable flight commands. Clearly, the degree of complexity in modeling the aircraft dynamics and its flight control systems affects the optimal strategy generated by the planner. The actual trajectory flown by the aircraft depends upon the accuracy in modeling its dynamic equations and is altered by varying the models of the control systems.

This thesis investigates the fidelity of the flight control systems needed in the trajectory planner. The disadvantage of very complex modeling of the control systems is an increased computational burden, and hence an untimely generation of the optimal commands. Such sluggishness may cause the aircraft to fly a trajectory leading to radar detection or missile sites. However, oversimplified models also tend to substantially deviate the aircraft from the optimal flight path and expose it to similar threats. Therefore, it is of interest to determine the minimum degree of complexity of the flight control systems required by the trajectory planner.

Another issue discussed in this thesis is the monitoring of the position and velocity of the aircraft. If such monitoring is absent between every set of two waypoints, the actual aircraft trajectory will be directly affected by wind shears and discrete gusts. Determination of the need for position and velocity feedbacks is predicated on the aircraft responses to such disturbances.

1.3 Thesis Organization

Towards the goal of achieving the previous objectives, chapter 2 discusses the designs of the flight control systems using full aircraft dynamics. Motives for dealing with full dynamics are presented. Performance limits and response characteristics of the control systems are studied and evaluated. In chapter 3, the effects of stochastic wind disturbances are addressed. The aircraft responses to wind gusts characterized

by their Dryden spectra are determined. Deterministic models of wind gusts are described in chapter 4. The question of continuous monitoring of position and velocity is also addressed. Command updates based on position and velocity feedbacks and the resulting aircraft responses are discussed in chapter 5. Flight path errors due to wind disturbances and model simplification are examined. The required degree of complexity in the models of the control systems is also presented. Finally, the results are summarized in chapter 6. Also presented there, are recommendations and directions for further research.

Chapter 2

Flight Control Systems Designs

2.1 Usage of Full Aircraft Dynamics

The objective of this thesis is to determine how complex the models of the flight control systems in the optimal trajectory planner need to be. Having this in mind, it is important to investigate the ability of the aircraft to follow the optimal trajectory. If the flight control systems are not well modeled, the actual aircraft trajectory will deviate from that predicted by the planner. The susceptibility of the airplane to be detected by radar will increase and render the mission more dangerous and harder to accomplish.

On the other hand, increasing the complexity of the models of the flight control systems may prevent the trajectory planner from converging to the optimal commands on time. That is, after one waypoint is passed, commands to steer the aircraft to the next waypoint, while minimizing a certain risk function, may not be available. When the aircraft is flying over a rough terrain with steep hills or narrow valleys, the timely availability of the flight commands will be crucial to the success of the mission.

Using full aircraft dynamics will enable us to compare complex versus simplified models. Subsequently, we can determine the least complex the flight control systems need to be based on the aircraft responses to commands and wind disturbances.

Another motive to deal with full aircraft dynamics is the determination of the need for continuous monitoring of position and velocity. Wind gusts and wind shears are

widespread in the atmosphere. They form the major source of disturbances which produce significant trajectory deviations. Since the aircraft in this research is assumed to be flying at 200 feet above the ground, deviations of 25 feet or larger are of concern and would necessitate that position and velocity be monitored continuously. As will be seen later, position and velocity feedbacks proved to be necessary.

2.2   Equations of Motion

The equations of motion of an aircraft referred to the stability axes system(figure 2-3) are given by :

$$X - mg\sin\Theta = m(\dot{U} + QW - RV) \tag{2.1}$$

$$Y + mg\cos\Theta\sin\Phi = m(\dot{V} + RU - PW) \tag{2.2}$$

$$Z + mg\cos\Theta\cos\Phi = m(\dot{W} + PV - QU) \tag{2.3}$$

$$P = \dot{\Phi} - \dot{\Psi}\sin\Theta \tag{2.4}$$

$$Q = \dot{\Theta}\cos\Phi + \dot{\Psi}\cos\Theta\sin\Phi \tag{2.5}$$

$$R = \dot{\Psi}\cos\Theta\cos\Phi - \dot{\Theta}\sin\Phi \tag{2.6}$$

where

(X,Y,Z) = components of aerodynamic forces, in lb

(U,V,W) = components of velocity vector, in ft/sec

(P,Q,R) = components of angular velocity vector, in radians/sec

(Θ, Ψ, Φ) = Euler angles, in radians

A convenient way to linearize the above equations is to use the small disturbance theory. The total motion can be considered as composed of two parts : an average or mean motion that is representative of the operating point, and a dynamic motion that accounts for small perturbations about the mean motion. For a steady, level flight, the perturbed equations of motion decouple into two sets of equations describing the

15

longitudinal and the lateral motions of the aircraft. This decoupling property aids in designing the longitudinal and the lateral flight control systems independently.

In this thesis, the characteristics of the A4D fighter aircraft are used. The flight is assumed steady and level and the equations of motion below correspond to an altitude of 200 feet and a nominal speed of 750 feet/second. The perturbed longitudinal equations are given by :

$$\dot{u} = -0.0097u + 0.0184\alpha - 0.562\theta + 2\delta_T + 0.0097u_g - 0.0016w_g \qquad (2.7)$$

$$\dot{\alpha} = -0.0083u - 1.43\alpha + q - 0.1057\delta_e + 0.0083u_g + 0.1238w_g \qquad (2.8)$$

$$\dot{q} = 0.0071u - 14.256\alpha - 2.778q - 26.01\delta_e + 0.000224\delta_T - 0.0071u_g + 1.2376w_g - 0.0917\dot{w}_g \qquad (2.9)$$

$$\dot{\theta} = q \qquad (2.10)$$

$$a_N = U_0(\dot{\alpha} - q) \qquad (2.11)$$

where

u = perturbed forward velocity, in *ft/sec*

α = perturbed angle of attack, in *degrees*

q = perturbed pitch rate, in *deg/sec*

θ = perturbed pitch angle in *degrees*

a_N = perturbed normal acceleration in *ft/sec²*

δ_e = perturbed elevator deflection, in *degrees*

δ_T = perturbed throttle angle, in *degrees*

u_g = forward component of wind velocity, in *ft/sec*

w_g = vertical component of wind velocity, in *ft/sec*

The perturbed lateral equations of motion corresponding to the same flight conditions are given by :

$$\dot{v} = -0.0829v + 0.562\phi - 11.5192r - 0.0064p + 0.0387\delta_a + 0.0829v_g \qquad (2.12)$$

$$\dot{p} = -0.3953v + 0.1717r - 1.7269p + 27.4428\delta_a + 0.3953v_g + 0.3667\dot{v}_g + 97.3627p_g \qquad (2.13)$$

16

$$\dot{r} = 0.2922v - 0.0893r - 0.2922v_g + 0.0083\dot{v}_g + 3.7471p_g \qquad (2.14)$$

$$\dot{\phi} = p \qquad (2.15)$$

where

v = perturbed side velocity, in *ft/sec*

p = perturbed roll rate, in *deg/sec*

r = perturbed yaw rate, in *deg/sec*

ϕ = roll angle, in *degrees*

δ_a = aileron deflection, in *degrees*

v_g = lateral component of wind velocity, in *ft/sec*

p_g = roll due to gradient of vertical component of wind velocity along the span of the aircraft, in *1/sec*

Since the aircraft is inherently stable in yaw, the coordination between the aileron deflection, δ_a, and the rudder deflection, δ_r, was chosen to cancel out the effect of the aileron and the roll rate, p, on the yaw rate, r. In this case, the rudder deflection is given by :

$$\delta_r = -0.048p + 0.2895\delta_a \qquad (2.16)$$

The longitudinal and the lateral equations of motion are referred to the stability axes system of the aircraft (figure 2-3). This axes system moves with the aircraft. It consists of the x-axis pointing in the relative wind direction. The y-axis points along the right wing of the aircraft. The direction of the z-axis is given by the following cross product : $l_z = l_x \times l_y$, where l_x and l_y are the unit vectors along the x and y axes respectively. The z-axis is positive down in level flights

Because of the decoupling property, it is possible to design the longitudinal and the lateral flight control systems independently. The decoupling applies to level flights (i.e. $\Phi_0 = 0$). However, even for large nominal values of the roll angle, ($\Phi_0 = \bigcirc(\pi/2)$), the designed flight control systems were insensitive to the nominal value of the roll

angle. In this context, the equations of motion were linearized about a nonzero nominal value of the roll angle and the control law designed for $\Phi_0 = 0$ was applied. It was found that the locations of the closed loop poles were the same as those of the closed loop poles corresponding to a linearization about the level flight condition. Therefore, it is safe to state that the flight control systems designed about $\Phi_0 = 0$ will lead to stable control systems for arbitrary roll angle values.

2.3 Design of Flight Control Systems

2.3.1 Longitudinal Case

According to the conclusions drawn in the previous section, the command following loop design of the longitudinal flight control system was performed independently from the lateral one. Several motion variables are candidates for the command input such as the pitch angle, θ, or the flight path angle, $\gamma = \alpha - \theta$. However, based on the results of previous works, the normal acceleration, a_N, was determined to be the most suitable [1, 2].

In the flight control system design, the elevator deflection, δ_e, and the throttle angle, δ_T, were selected as the control variables. In addition to the normal acceleration, a_{N_c}, the forward velocity, u_c, was also chosen as a command variable. The availability of the throttle deflection as a command variable offers the advantage of a concurrent thrust control system design.

There is no inherent integrator between the elevator deflection, δ_e, and the normal acceleration, a_N. The lack of such an integrator prevents the normal acceleration from following a step command input with zero steady state error. Therefore, the command loop must be augmented by integrators in the forward path to eliminate such steady state errors (see figure 2-1). In Figure 2-1, G_I and G_P designate the integral and proportional gain matrices associated with the two reference command variables, a_{N_c} and u_c. G_{long} represents the gain matrix corresponding to the remaining longitudinal state variables. The selection of G_I, G_P, and G_{long} was done by using the
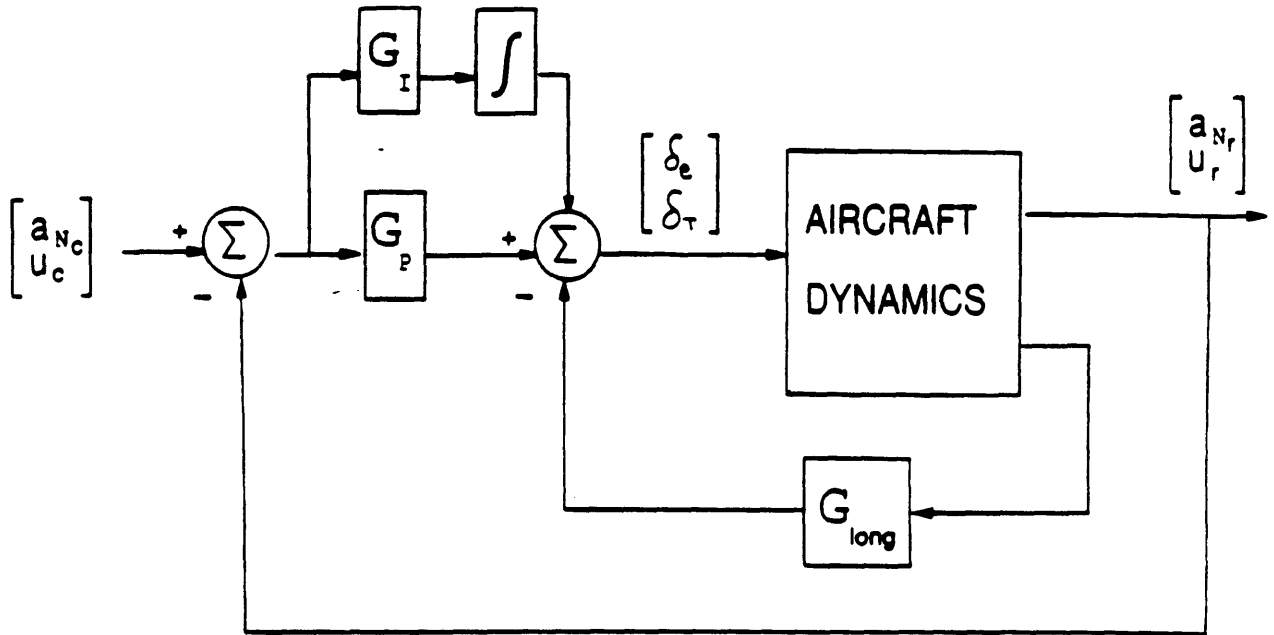
18

Figure 2-1: Normal Acceleration Command Loop

linear quadratic regulator approach. In this setting, the output variables that must track the reference command variables must be measured to form the error vector, $\underline{e}$, the difference between the reference command variables and the output variables.

The perturbed longitudinal equations of motion can be written in the following state space form :

$$\dot{\underline{x}} = A\underline{x} + B\underline{u} \tag{2.17}$$

$$\underline{y} = C\underline{x} \tag{2.18}$$

where

$\underline{x}^T = [\underline{z}^T \ a_N \ u \ \alpha \ \theta \ q]$

$\dot{\underline{z}} = \underline{y}$

$\underline{u}^T = [\delta_e \ \delta_T]$

$\underline{y}^T = [a_N \ u]$

The feedback gain matrices G_I, G_P, and G_{long} were selected to minimize a cost func-

tion of the form :

$$J = \int_0^\infty [\underline{x}^T Q \underline{x} + \underline{u}^T R \underline{u}] dt \qquad (2.19)$$

Q and R are diagonal, penalty matrices. Their entries were picked to obtain an acceptable normal acceleration step response. For instance, the normal acceleration step response is characterized by an undershoot. This undershoot is the result of a non-minimum phase zero present in the transfer function having the elevator deflection, δ_e, as the input, and the normal acceleration, a_N, as the output. If the percentage of the undershoot to a step input was unacceptable, (i.e. greater than 20%), the elevator deflection would be more heavily penalized. Similarly, if the response error or the settling time to a normal acceleration step input were too large, the penalty on the normal acceleration state variable would be increased. The response characteristics to a step input in the normal acceleration command are shown in figure 2-4.

2.3.2 Performance Limits

The presence of a non-minimum phase zero in the normal acceleration command loop sets inherent performance limits in the design process. Such a limitation can be seen by analyzing the sensitivity function. If the control system is described in a state space form, see equations (2.17) and (2.18), the sensitivity function, $S(j\omega) = (I + C(j\omega I - A)^{-1}B)^{-1}$, describes the effect of external disturbances on the output, $\underline{y}$. In general, the energy content of the external disturbances is concentrated in low frequency ranges. The aircraft is affected most by the long wavelength components of air turbulence. To minimize the effect of wind gusts on the tracking variable, a_N, the magnitude of $S(j\omega)$ must be small over the bandwidth of the system (i.e. $\|S(j\omega)\| \ll 1$ at low frequencies).

However, the magnitude of the sensitivity function cannot be made arbitrarily small due to the presence of the non-minimum phase zero. In fact, the magnitude of the sensitivity function at the frequency of the non-minimum phase zero is 1.

20

Using the concept of subharmonic functions [6], quantitative limits on the sensitivity function can be established.

If σ_0 designates the frequency of the non-minimum phase zero and if $\log \|S(j\omega)\| \leq -M$ for $| \omega | \leq \omega_B$, then the sensitivity function will be constrained to :

$$\log \sup_{\omega \in \Re} \|S(j\omega)\| \geq M \frac{\theta}{\pi - \theta} \tag{2.20}$$

This result can be attributed to the fact that $\log \bar{\sigma}[S(j\omega)]$ is a subharmonic function. $\bar{\sigma}$ designates the maximum singular value. In equation (2.20), M is an arbitrary constant describing the effect of disturbance rejection. θ is given by : $\theta = 2\arctan(\omega_B/\sigma_0)$. Unless $\omega_B \ll \sigma_0$, the sensitivity function will be characterized by a substantial peak.

Figure (2-6) clearly depicts the same attribute. The normal acceleration command loop has a non-minimum phase zero at a frequency of $\sigma_0 = 19 rad/sec$. If the magnitude of the sensitivity is decreased in the low frequency range, the severity of the peak at higher frequencies will be more pronounced.

Another performance limit is imposed by the physical limits of the elevator. It is necessary to maintain the elevator deflection below 25^0 to avoid stall characteristics at the elevator. As a consequence, the normal acceleration response cannot track the reference command arbitrarily fast, leading to limits on the response time of the normal acceleration.

2.3.3 Lateral Case

The roll angle command following loop is shown in figure 2-2. The aileron deflection, δ_a, was selected as the control variable. The coordination between aileron and rudder deflections is according to equation (2.16). The scalar gain, g, is the proportional gain associated with the roll angle. G_{lat}, a gain matrix, is associated with the remaining lateral state variables, i.e. the side velocity, v, the roll rate, p, and the yaw rate, r. Both gains, g and G_{lat}, were evaluated by using the linear quadratic approach.
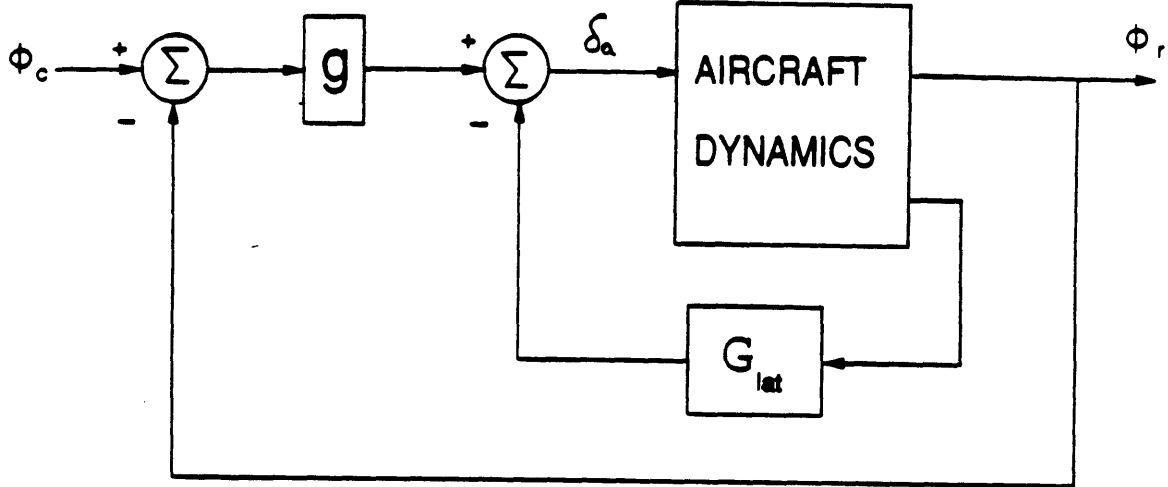
Figure 2-2: Roll Angle Command Following Loop

A quadratic cost form similar to the one used in the longitudinal loop design was minimized; and the corresponding feedback gains were chosen to lead to an acceptable settling time in the roll angle response to a reference step input. Because of the presence of inherent integrators in the forward loop, no artificial augmentation is needed. The aircraft's response and the aileron deflection resulting from a roll angle step command are shown in figures 2-5.

Although no non-minimum phase zero is present in the roll angle command loop, performance limits exist. They are attributed to the physical constraints imposed by the aileron deflection. Such constraints are similar to those associated with the elevator deflection, and they prevent the roll angle from tracking a step command input arbitrarily fast. In addition, complete rejection of arbitrarily large output disturbances over the bandwidth of the system cannot be achieved because of these physical constraints.

RELATIVE
WIND
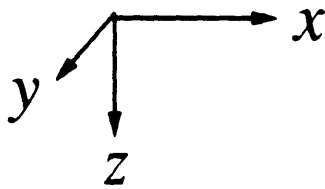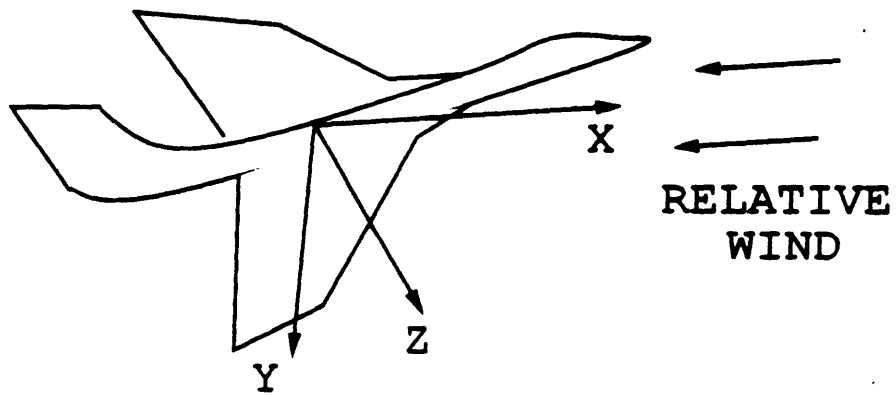
(X,Y,Z) STABILITY
AXES SYSTEM

(x,y,z) INERTIAL
COORDINATES SYSTEM
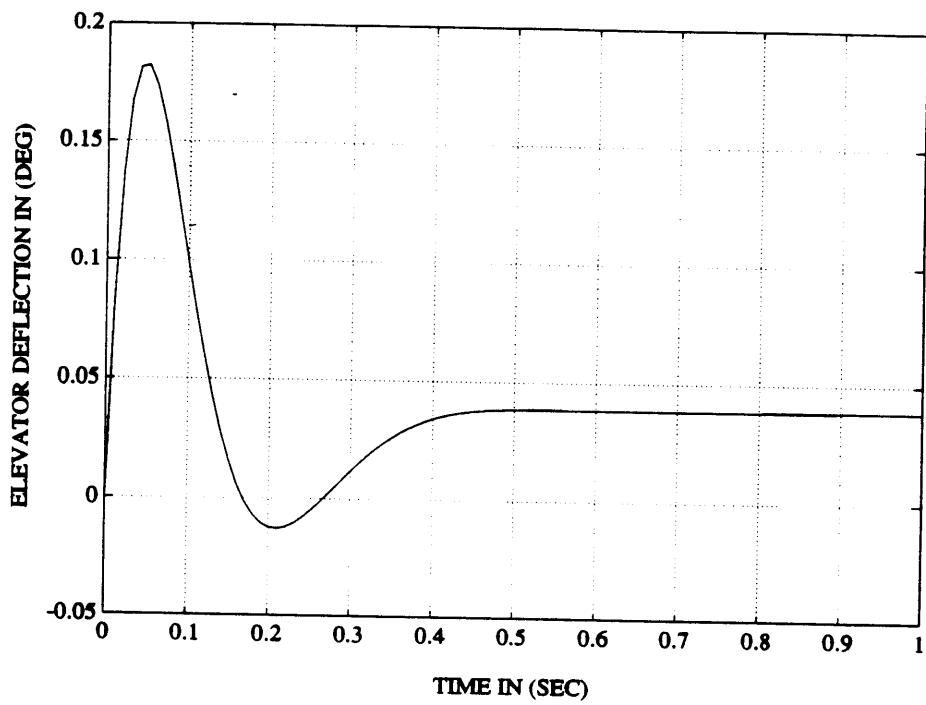
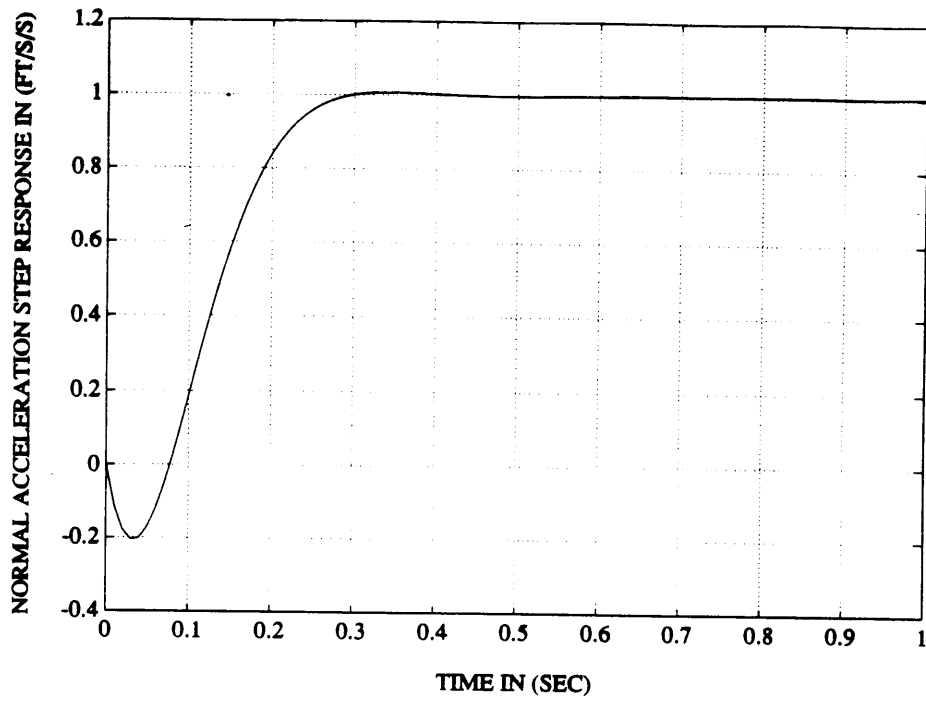Figure 2-3: Aircraft Stability Axes System

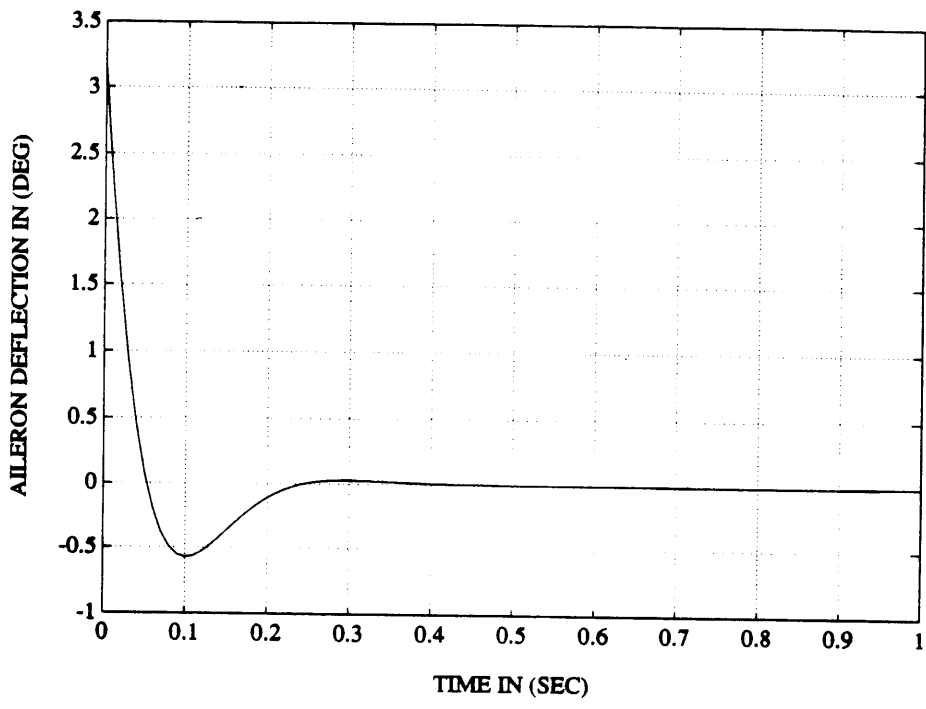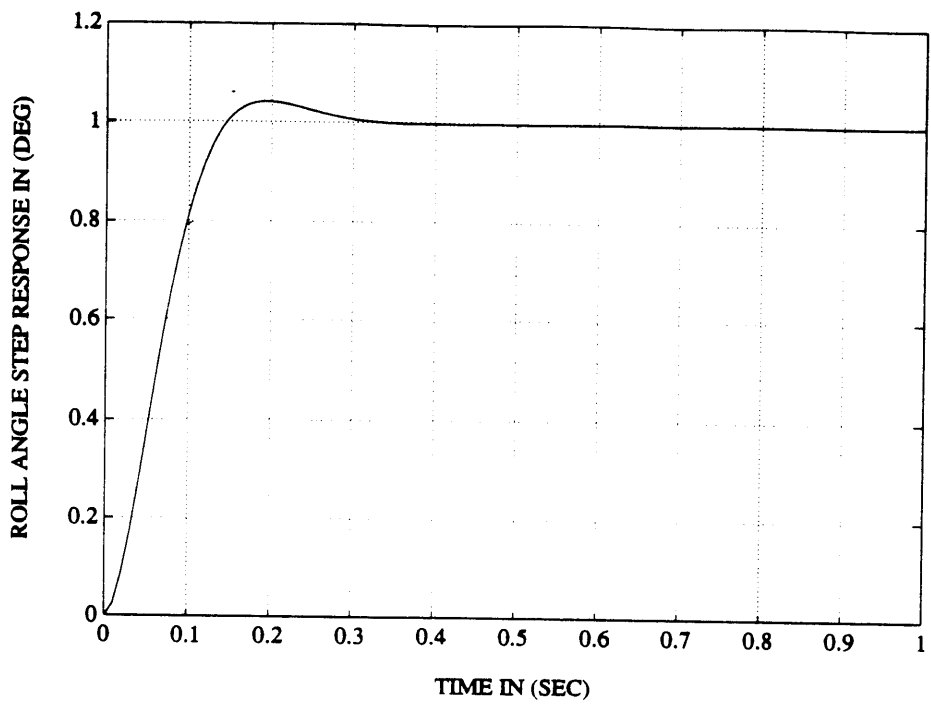Figure 2-4: Responses to a Normal Acceleration Step Input
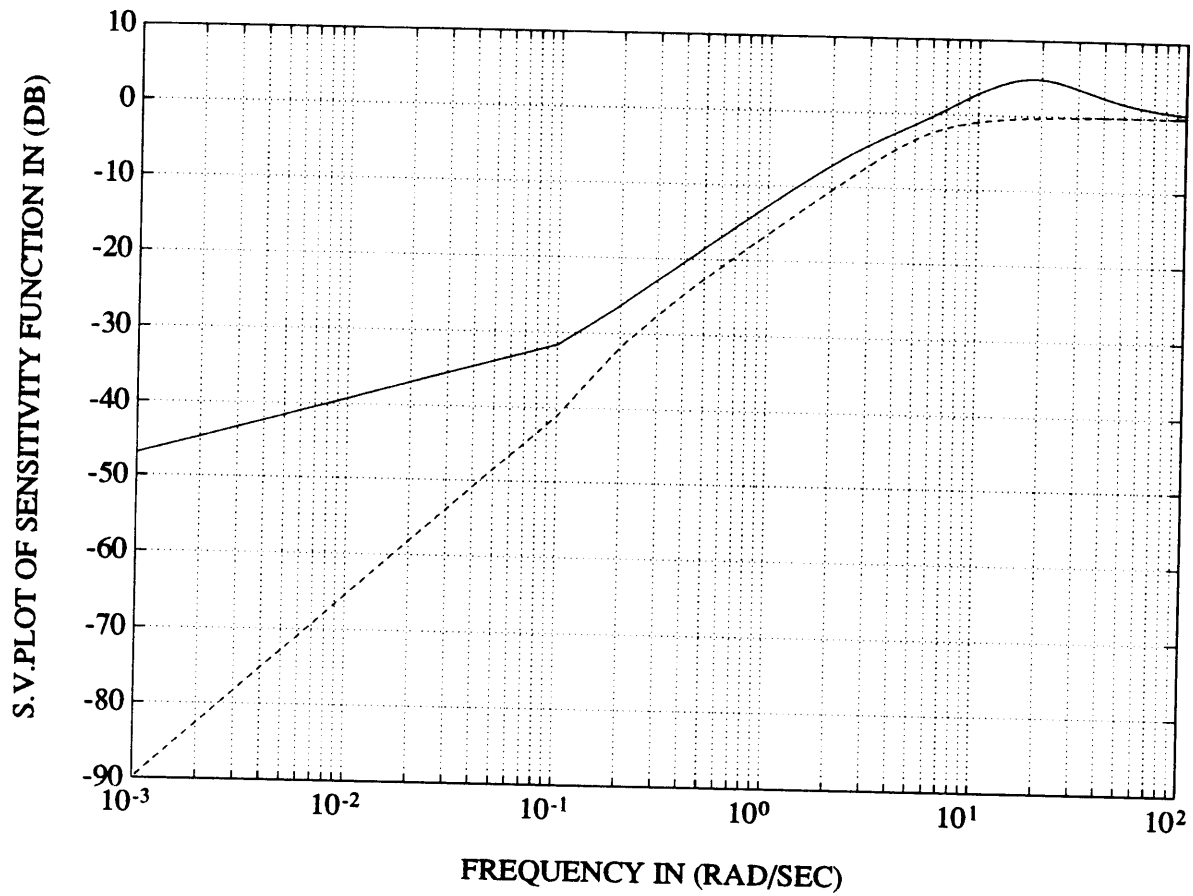
Figure 2-5: Responses to a Roll Angle Step Input

Figure 2-6: Singular Value Plot of Longitudinal System Sensitivity Function

Chapter 3

Stochastic Analysis

If the atmosphere were uniform and wind disturbances were non existent, the designed flight control systems would be satisfactory. No further augmentation to the command loops would be needed; and the aircraft would closely follow the optimal trajectory. However, it is known that the atmosphere is in constant motion. Gradients in temperature, pressure, and velocity give rise to air turbulence.

Since the aircraft is flying very close to the ground, the most serious effects of wind disturbances are those that cause the aircraft to lose lift and altitude. Of equal importance are the wind disturbances that lead to significant lateral deviations from the minimum risk flight path produced by the planner.

3.1 Atmospheric Turbulence Assumptions

In this thesis, air turbulence is assumed to take the form of individual patches characterized by their intensity. The intensity in each patch describes the root mean square of any of the turbulent velocity components. The spectrum or the frequency content of the turbulence in each patch is related to the intensity.

Another assumption often made about air turbulence is that of isotropy. Statistical properties are assumed to be independent of orientation of axes. At low altitudes, it is proved that the atmosphere is anisotropic. Lack of isotropy at low altitudes implies that the statistical properties of the turbulence differ among the three turbulent

27

velocity components (u_g, v_g, w_g). Furthermore, the absence of isotropy leads to the existence of statistical cross correlations among the three velocity components. For simplicity however, it is assumed that these cross correlations are negligible.

Taylor's hypothesis is also assumed in this thesis. The hypothesis states that time variations are statistically equivalent to distance variations in traversing the turbulence field. In this case, the temporal frequency sensed by the aircraft can be related to the spatial frequency of the turbulence according to the following equation :

$$\omega = V\Omega \tag{3.1}$$

where ω is the temporal frequency in rad/sec, V is the aircraft's velocity in feet/sec through the turbulence field, and Ω is the spatial frequency of the air turbulence waves in rad/feet.

Another implication of Taylor's hypothesis is that turbulence-induced aircraft responses result only from the motion of the aircraft relative to the turbulence field. In this case, statistical properties of the turbulence as sensed by the aircraft are independent of time. Consequently, stationary statistical methods can be used in analysis.

In this thesis, the results of wind disturbance analysis apply only to the long wavelength components of air turbulence. The wavelengths were assumed to be at least as large as eight times the length of the aircraft. As a consequence, the variation of the wind gust velocity along the length or the span of the aircraft is approximately linear. To account for the effects of short wavelength turbulence, equivalent aerodynamic force and moment terms must be calculated empirically.

3.2 Dryden Gust Spectra

There are two models that describe the spectra of air turbulence. They are known as the von Karman and Dryden spectra. Both of these models satisfy all the mathematical requirements for isotropy. Although the von Karman spectra describe air turbulence behavior more accurately, the Dryden gust spectra were analyzed in this research. The selection of the Dryden gust spectra was based upon their rational

form; leading to significant simplification in analysis and computation. The gust spectra associated with the three wind velocity components (u_g, v_g, w_g) are given by the following equations :

$$\Phi_{u_g}(\omega) = \sigma_u^2 \frac{2L_u}{U_0} \frac{1}{[1 + (L_u\omega/U_0)^2]} \qquad (3.2)$$

$$\Phi_{v_g}(\omega) = \sigma_v^2 \frac{L_v}{U_0} \frac{1 + 3(L_v\omega/U_0)^2}{[1 + (L_v\omega/U_0)^2]^2} \qquad (3.3)$$

$$\Phi_{w_g}(\omega) = \sigma_w^2 \frac{L_w}{U_0} \frac{1 + 3(L_w\omega/U_0)^2}{[1 + (L_w\omega/U_0)^2]^2} \qquad (3.4)$$

Equations (3.2, 3.3, 3.4) describe the gust spectra directly in terms of the temporal frequency, ω, as sensed by the aircraft. In these equations, U_0 designates the nominal velocity of the aircraft, 750 ft/sec. σ_i, $(i = u_g, v_g, w_g)$, represents the intensity associated with the corresponding gust. L_i $(i = u, v, w)$ are scale lengths related to the altitude of the aircraft and the severity of air turbulence (e.g. clear air turbulence or thunderstorm turbulence). Equations (3.2, 3.3, 3.4) are defined such that $\sigma_i^2 = \frac{1}{\pi} \int_0^\infty \Phi_i(\omega)d\omega$. In the stochastic simulation, a gust intensity of 5 feet/sec was used. It was felt that air turbulence having such intensity is not uncommon at the aircraft's nominal altitude, 200 feet. In fact, the probability of equaling or exceeding a 5 feet/sec intensity at 200 feet is 0.08 [4]. Clear air turbulence was also assumed in the simulation.

Gust velocity gradients along the span of the aircraft produce substantial rolling motions. The spectrum associated with the variations of w_g along the span of the aircraft is given by :

$$\Phi_{p_g}(\omega) = \sigma_w^2 (\frac{\pi}{4b})^{1/3} \frac{0.8}{U_0 L_w^{2/3}[1 + (4b\omega/\pi U_0)^2]} \qquad (3.5)$$

29

where b is the aircraft wing span.

3.3 Propagation of State Covariances

The method of stochastically simulating air turbulence was to pass a Gaussian white noise through a filter (see figure 3-1). The filter shapes the random output such that it has certain statistical properties characteristic of the atmospheric turbulence to be simulated. The two statistical parameters which are reproduced are the turbulence intensity, σ_i, and the frequency content, Φ_i, through the turbulence energy spectrum. The random effect of air turbulence on the aircraft can be evaluated by propagating the covariances of the state variables of interest in time. In general, a stochastic process can be described by a linear differential equation driven by white noise so that the power spectral density of the response is the same as the power spectral density of the original stochastic process.

It is of interest to examine the aircraft stochastic response after implementing the designs of the flight control systems. The aircraft equations of motion can be combined with the differential equations corresponding to the shaping filters. The resulting equations can be conveniently arranged in the following state space form :

$$\dot{\underline{x}} = A\underline{x} + B\underline{w} \tag{3.6}$$

$$\underline{y} = C\underline{x} \tag{3.7}$$

where the correlation of $\underline{w}$ is : $E[\underline{w}(t)\underline{w}^T(t-\tau)] = I\delta(\tau)$. Since equation(3.6) is driven by white noise, the propagation of the state covariances is given by the matrix Lyapunov equation :

$$\dot{P} = AP + PA^T + BB^T \tag{3.8}$$

where P represents the state covariance matrix. Integrating equation(3.8) forward in

time with zero initial conditions (i.e. $P(0) = 0$), the variations of the state covariances with respect to time can be determined. Figure 3-2 shows how the standard deviation of the normal acceleration evolves with time. Similar standard deviation plots for the angle of attack, the roll angle, and the side velocity are shown in figures 3-3, 3-4, 3-5 respectively.

To appreciate the effect of the random wind turbulence on the aircraft trajectory, standard deviations of the aircraft's position and velocity seen in a fixed axes system should be evaluated. Towards this goal, a transformation between the aircraft's stability axes system and the inertial system must be performed. The components of the aircraft's velocity in the fixed axes system are given by :

$$dX/dt = U\cos\Theta\cos\Psi + V(\sin\Phi\sin\Theta\cos\Psi - \cos\Phi\sin\Psi) +$$
$$W(\cos\Phi\sin\theta\cos\Psi + \sin\Phi\sin\Psi) \tag{3.9}$$

$$dY/dt = U\cos\Theta\sin\Psi + V(\sin\Phi\sin\Theta\sin\Psi + \cos\Phi\cos\Psi) +$$
$$W(\cos\Phi\sin\Theta\sin\Psi - \sin\Phi\cos\Psi) \tag{3.10}$$

$$dZ/dt = -U\sin\Theta + V\sin\Phi\cos\Theta + W\cos\Phi\cos\Theta \tag{3.11}$$

Perturbing the motion variables about their nominal values (i.e. $U = U_0 + u, \Theta = \theta_0 + \theta$ etc.), and neglecting second and higher order terms, the perturbed inertial components of the aircraft's velocity are obtained :

$$dx/dt = (U_0 + u)\cos\theta_0 - U_0\theta\sin\theta_0 + w\sin\theta_0 \tag{3.12}$$

$$dy/dt = U_0\psi\cos\theta_0 + v \tag{3.13}$$

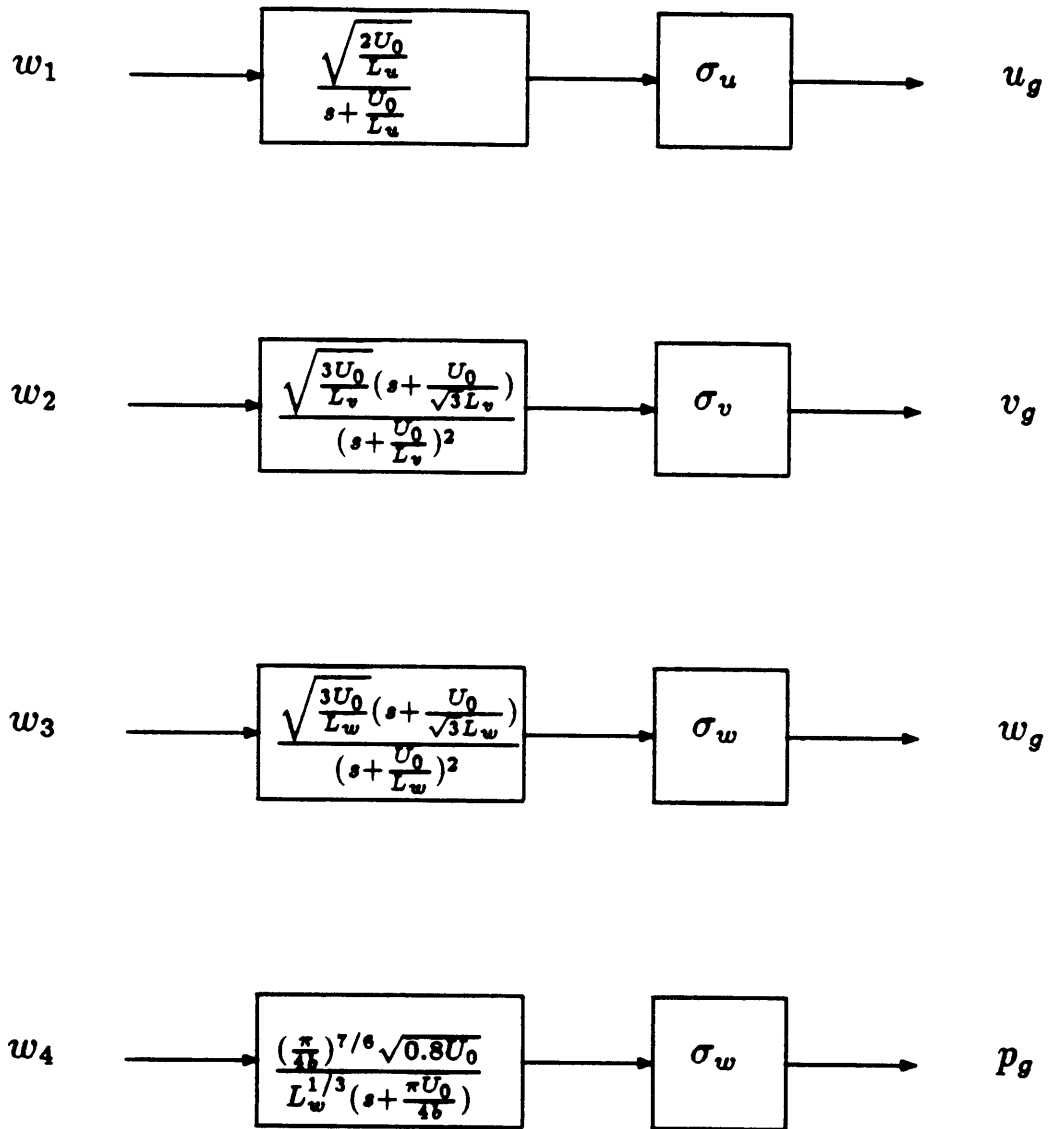$$dz/dt = -(U_0 + u)\sin\theta_0 - U_0\theta\cos\theta_0 + w\cos\theta_0 \tag{3.14}$$

The above equations, describing the transformation sought after, were arrived at as-

31

suming the reference flight conditions correspond to constant velocity and wings level flight, i.e. $\Phi_0 = 0$. This transformation can be written in a matrix form as : $\underline{v} = T\underline{x}$, where $\underline{v}^T = [dx/dt \ dy/dt \ dz/dt]$, $\underline{x}^T = [u \ v \ w \ \theta \ \psi]$. The covariances of the aircraft's velocity components in the inertial coordinates system are then given by :

$$V = TP'T^T \tag{3.15}$$

where P' is the covariance matrix of the states represented by the vector $\underline{x}$. The standard deviations of the aircraft's position in the fixed axes system represent the root mean square displacements from the optimal trajectory. Figures 3-6, 3-7, show the standard deviations of the lateral and vertical velocity components in the inertial coordinates system. The standard deviations of the lateral and vertical position components in the fixed axes system are illustrated in figures 3-8, 3-9 respectively. From a stochastic point of view, it is clear that position and velocity feedbacks are needed to compensate for the large deviations due to random air turbulence. As will be seen in the next chapter, the same conclusion is drawn regarding the effect of deterministic models of wind gusts on the aircraft's flight path.

$w_1 \longrightarrow \boxed{\dfrac{\sqrt{\frac{2U_0}{L_u}}}{s+\frac{U_0}{L_u}}} \longrightarrow \boxed{\sigma_u} \longrightarrow u_g$

$w_2 \longrightarrow \boxed{\dfrac{\sqrt{\frac{3U_0}{L_v}}\left(s+\frac{U_0}{\sqrt{3}L_v}\right)}{\left(s+\frac{U_0}{L_v}\right)^2}} \longrightarrow \boxed{\sigma_v} \longrightarrow v_g$

$w_3 \longrightarrow \boxed{\dfrac{\sqrt{\frac{3U_0}{L_w}}\left(s+\frac{U_0}{\sqrt{3}L_w}\right)}{\left(s+\frac{U_0}{L_w}\right)^2}} \longrightarrow \boxed{\sigma_w} \longrightarrow w_g$

$w_4 \longrightarrow \boxed{\dfrac{\left(\frac{\pi}{4b}\right)^{7/6}\sqrt{0.8U_0}}{L_w^{1/3}\left(s+\frac{\pi U_0}{4b}\right)}} \longrightarrow \boxed{\sigma_w} \longrightarrow p_g$

$w_i = $ **independent Gaussian white noise**

Figure 3-1: Stochastic Simulation of Air Turbulence
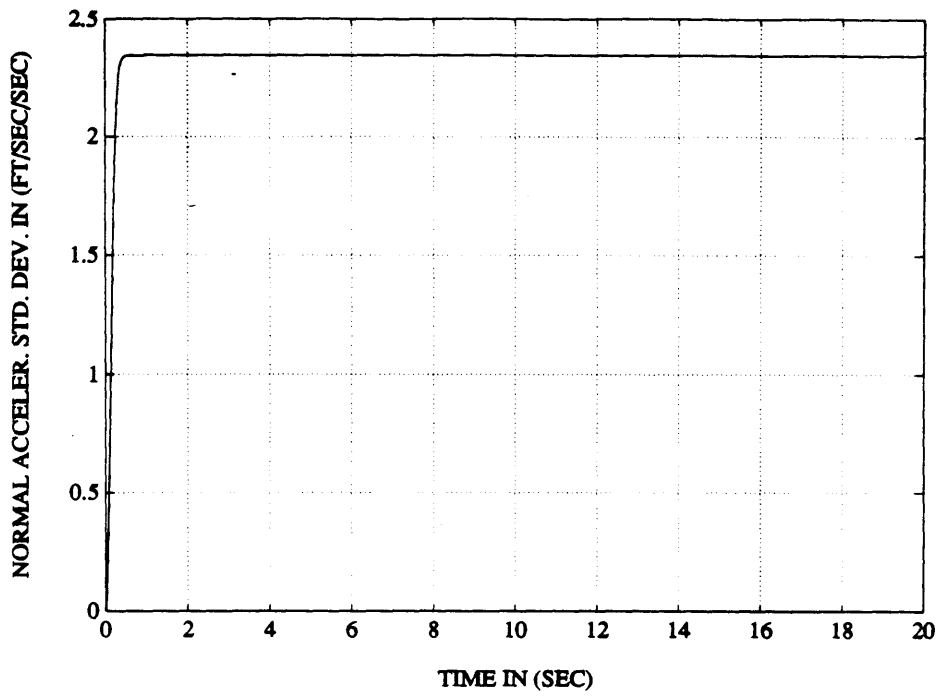
Figure 3-2: Normal Acceleration Standard Deviation Plot
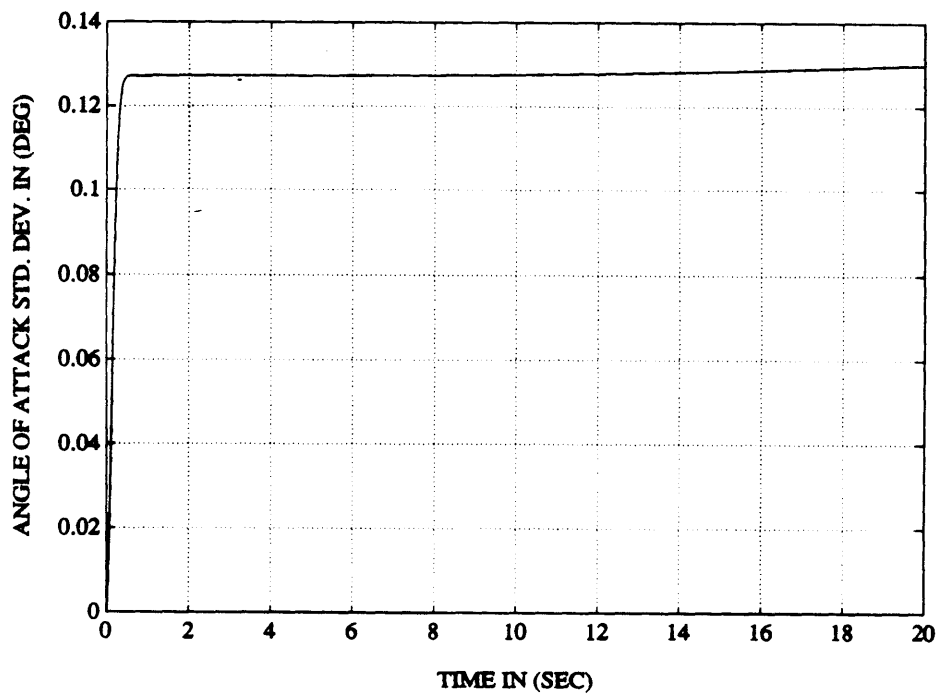
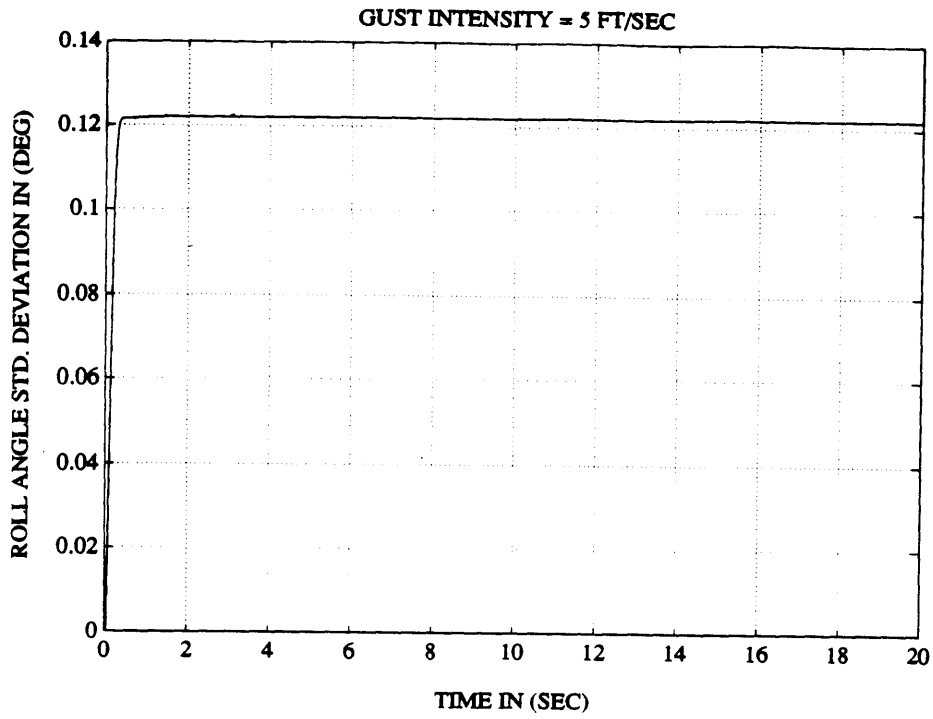Figure 3-3: Angle of Attack Standard Deviation Plot

34

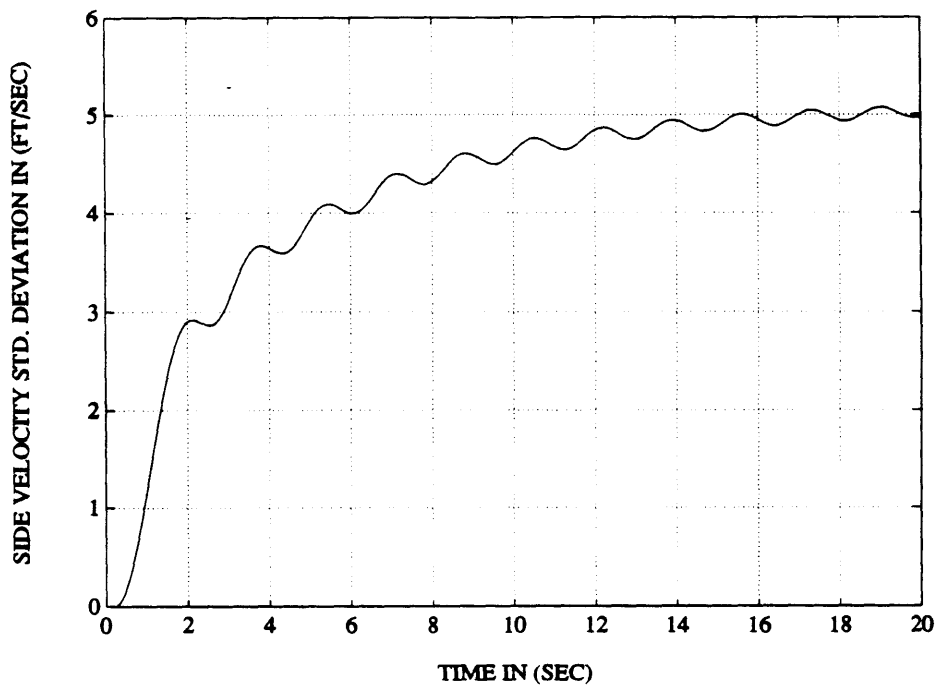Figure 3-4: Roll Angle Standard Deviation Plot

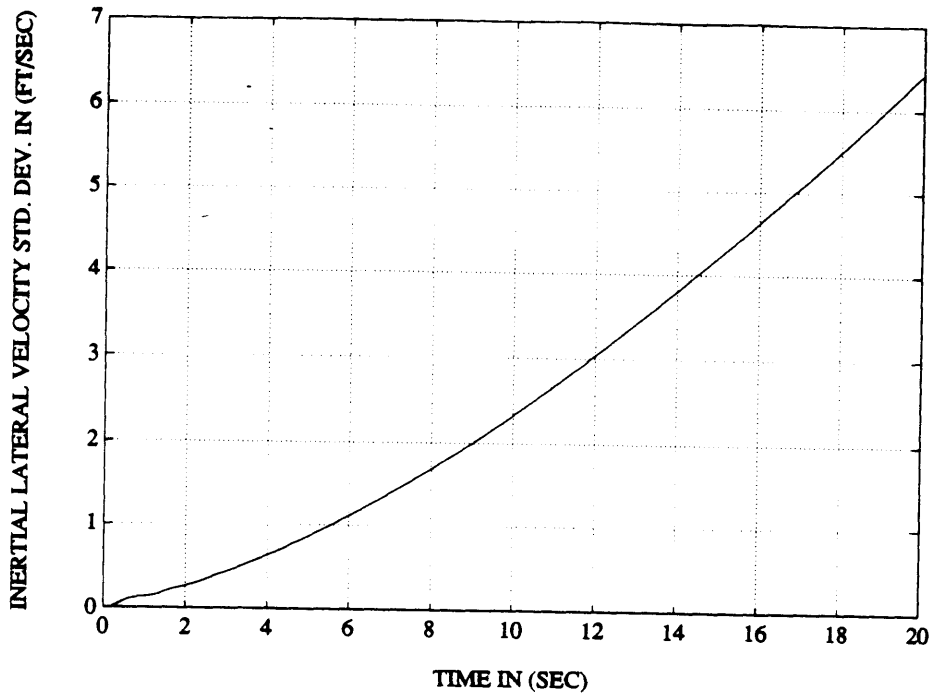Figure 3-5: Side Velocity Standard Deviation Plot

Figure 3-6: Inertial Lateral Velocity Standard Deviation Plot
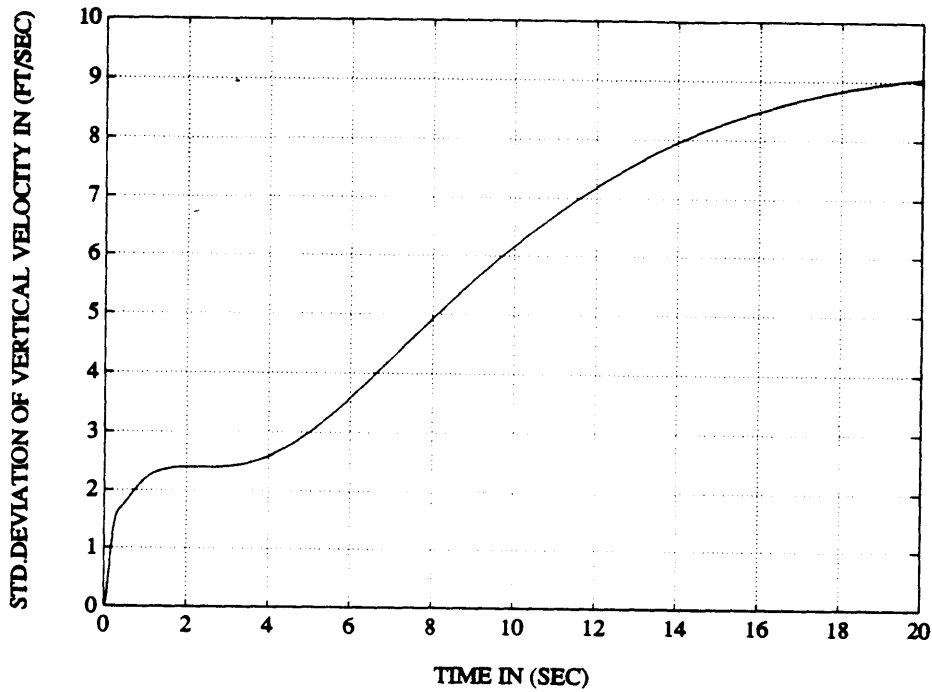

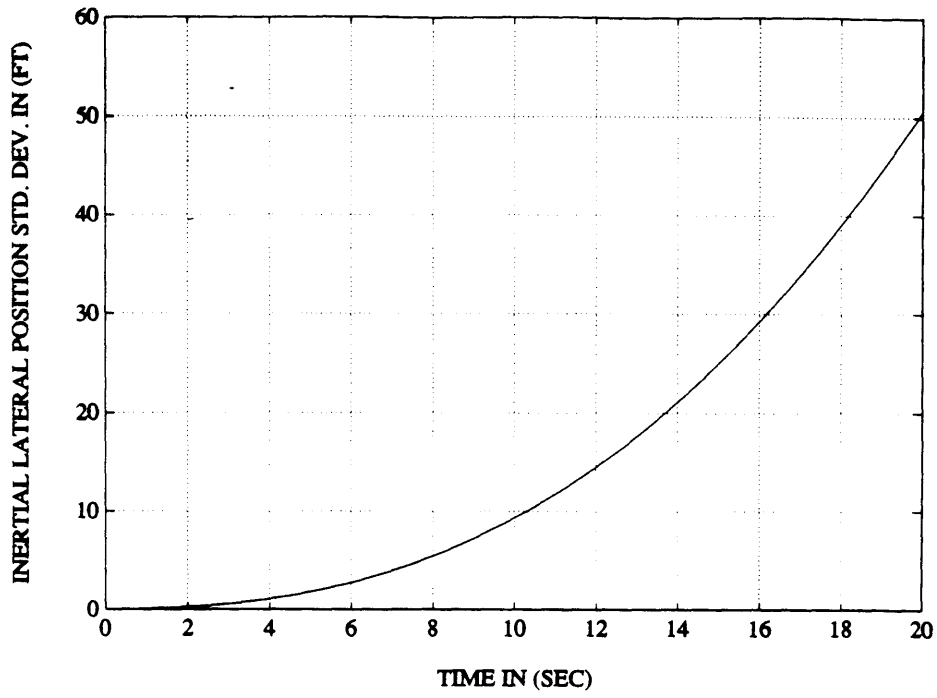Figure 3-7: Inertial Vertical Velocity Standard Deviation Plot

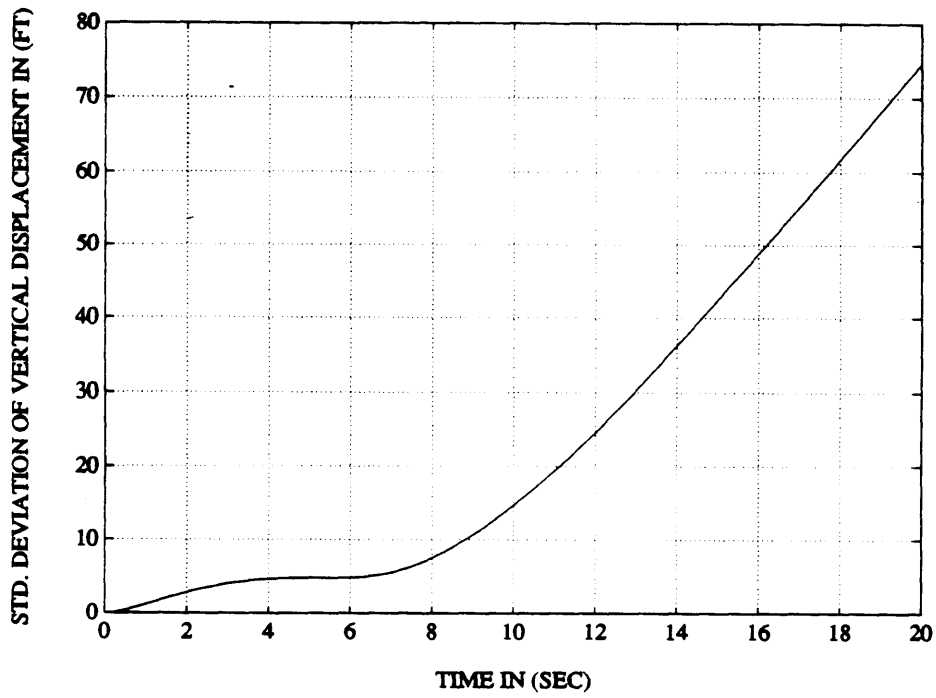Figure 3-8: Inertial Lateral Position Standard Deviation Plot

Figure 3-9: Inertial Vertical Position Standard Deviation Plot

37

Chapter 4

Deterministic Analysis

Meteorological circulations or terrain-induced airflows can on occasion induce large and rapidly changing variations in air velocity over small distances. These variations produce corresponding sudden changes in the relative flow of air over the aircraft's wings and other lifting surfaces, with attendant changes in the aircraft's actual flight path. In order to gain insight about the severity of ensuing trajectory deviations, deterministic models of air turbulence were analyzed and simulated.

4.1   Sharp-Edged Gusts

Separate air masses do not mix readily when they come into contact if they have different temperatures and humidity. Instead, the colder, more dense air mass passes below the warmer, less dense air mass. Consequent downdrafts result from the airflow between the two air masses. As the downdrafts approach the ground, they turn and move outwards along the Earth's surface. The velocity field depicting such air motion is shown in figure 4-1.

As the aircraft traverses through the downdraft, the effect of the wind gust it senses can be modeled as a sharp-edged gust (see figure 4-2). The time period during which the aircraft experiences air turbulence can be varied by changing the length of the gust, d. The intensity of the gust translates directly into the maximum amplitude, V_m, of the velocity of the gust model.
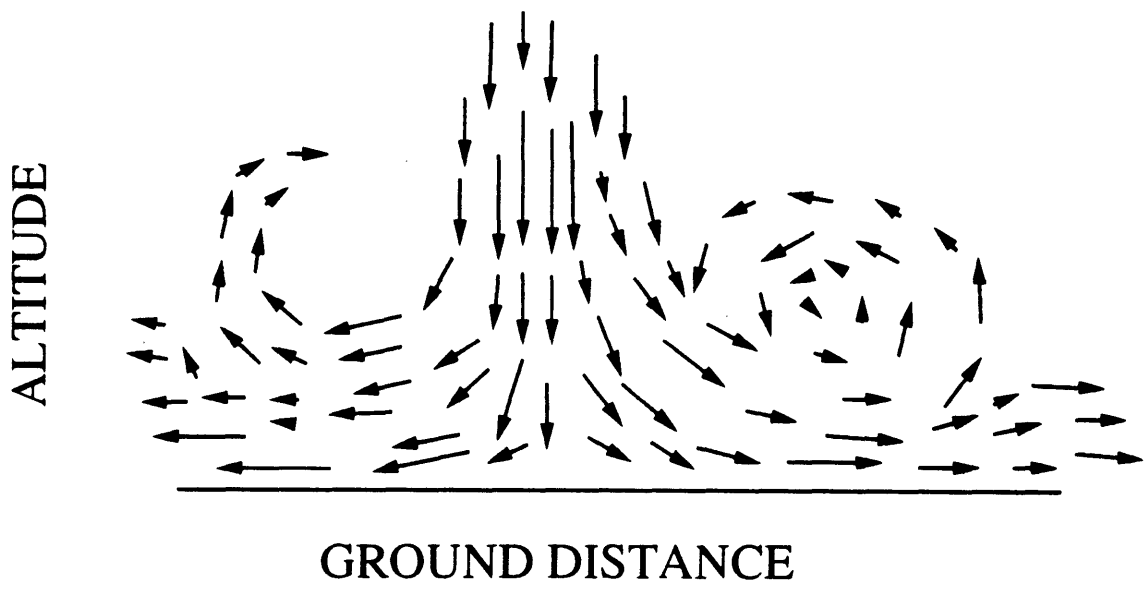
ALTITUDE

GROUND DISTANCE

Figure 4-1: Velocity Field of a Downdraft

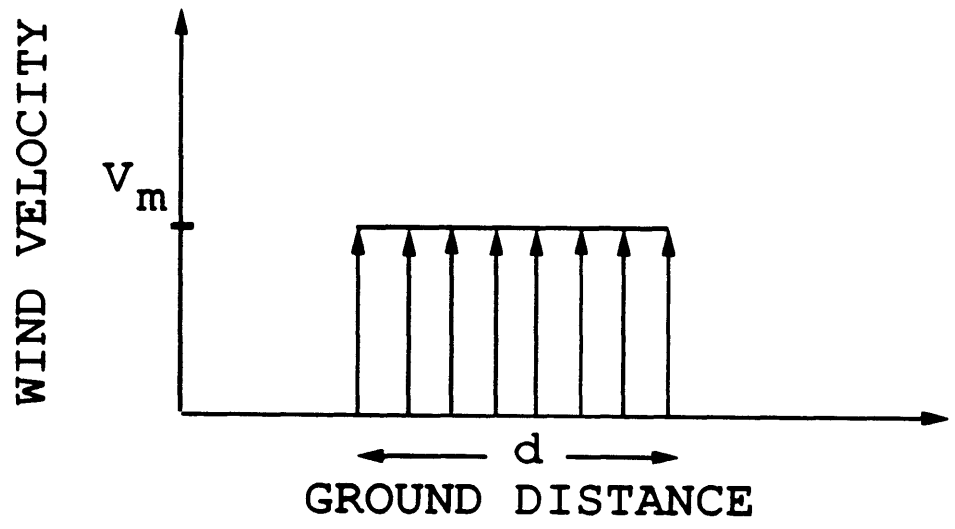WIND VELOCITY

V_m

d

GROUND DISTANCE
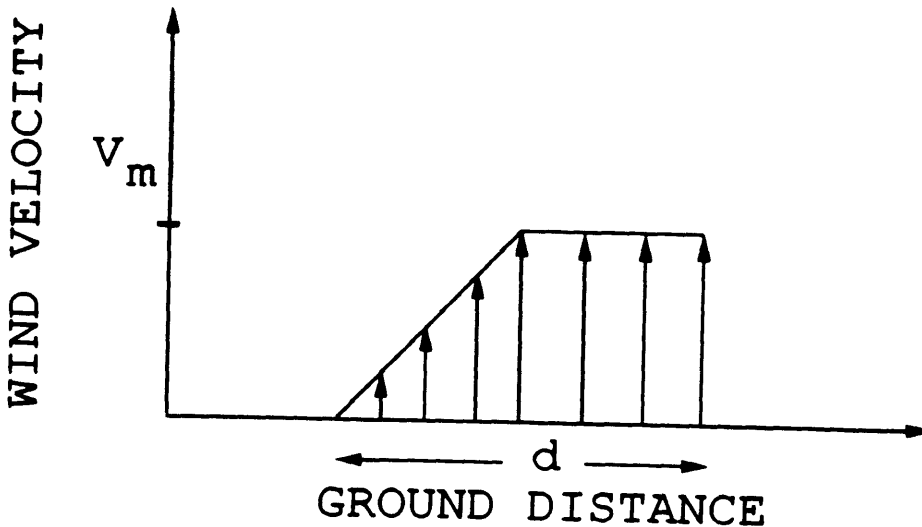
Figure 4-2: Sharp-Edged Gust Model

Figure 4-3: Wind Shear Model

4.2 Graded Gusts

Thunderstorms are critically important sources of low-altitude wind variability. The size and strength of the wind shears created depend on the properties of the thunderstorm as well as on the humidity and temperature of the atmosphere. The variations in wind speed are measured in the vertical and the horizontal directions. To describe such variations, a simple wind shear model was used in the simulation (see figure 4-3). In the first part of the model, the wind velocity varies linearly with the distance traversed. Once it reaches a maximum value, the wind velocity remains constant thereafter.

4.3 Discrete Gusts

Mountain terrain can cause significant low-altitude wind gusts, depending on the nature of the wind field. Hills with sharp dropoffs give rise to steady- state winds that break down into chaotic gusts. These strong, gusty winds at the Earth's surface produce low-altitude wind turbulence. As a consequence, they can compound the problem of following the nominal flight path predicted by the trajectory planner.
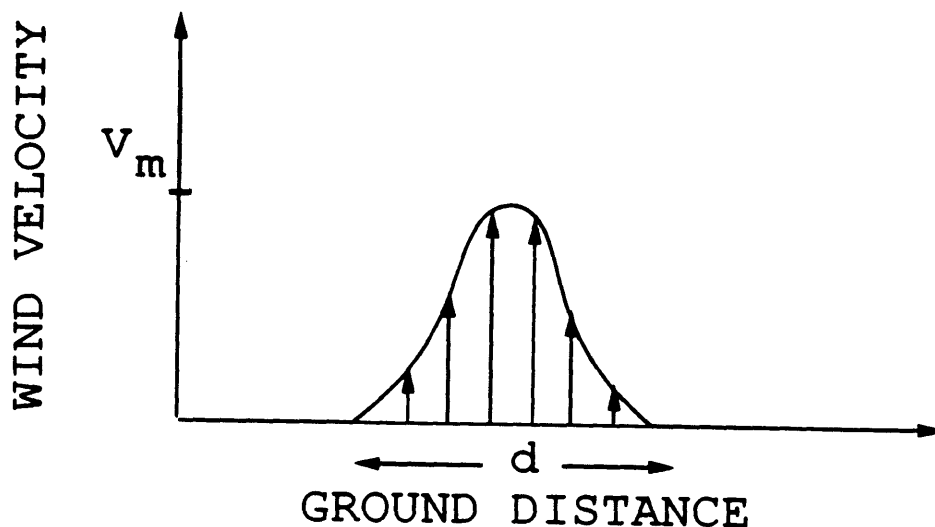
Figure 4-4: Discrete Gust Model

Because of the pulsing nature of terrain-induced winds, a "(1 - cos)" form was used to model their behavior (see figure 4-4). The sharpness of the encounter of the aircraft to such gusts can be altered by varying the width of the pulse. The intensity of the discrete gust is chosen by selecting the maximum amplitude of the wind pulse that would be more realistic based on wind data. In the simulation, a value of 5 ft/sec was chosen for the maximum amplitude of the wind gust. In clear air turbulence, the probability of equaling or exceeding such a value is 0.08 [4].

4.4   Aircraft Responses to Wind Gusts

The aircraft generates the aerodynamic forces that make flight possible by means of airspeed, which is the velocity of the aircraft relative to the surrounding air. A change in velocity of the surrounding air, or a wind gust, will cause a change in the aerodynamic forces on the aircraft. When air turbulence is encountered, there will be changes in components of wind along each of the aircraft's axes of motion. The wind component along the forward axis is a tailwind or headwind. The vertical axis has its associated updrafts or downdrafts; and the lateral axis has its associated crosswinds from the left or right.

41

Each of these wind components will produce a different response based on the aircraft's aerodynamic configuration. The effects of tailwinds or headwinds on the aircraft trajectory are not of major concern. The reason stems from the fact that the trajectory planner is made aware of the aircraft's position and velocity as each waypoint is passed. Any substantial loss of time can be made up by increasing the thrust over the next sets of waypoints. Instead, vertical and lateral wind gusts are the principal sources expected to cause significant flight deviations.

4.4.1   Response to Vertical Gusts

An updraft disturbs the airplane by increasing its angle of attack. This increased angle of attack increases lift and drag, which cause the aircraft to climb and decelerate. Assuming the presence of static stability, the increased lift causes the aircraft to pitch nose-down to reduce the angle of attack and to recover its original value.

The opposite situation, a downdraft, decreases the aircraft's angle of attack, thus reducing lift and causing it to sink. To appreciate the effect of air turbulence on the aircraft, a vertical sharp-edged gust of 5 ft/sec intensity was simulated. Figure 4-6 shows the nominal trajectory resulting from a normal acceleration step command. In the presence of a wind gust, it is clear that the trajectory deviations are significant and too large to be tolerable. To remedy this problem, position and velocity feedbacks will be needed.

4.4.2   Response to Lateral Gusts

Crosswinds and lateral wind shears act on the aircraft by generating side forces plus yawing and rolling moments. The initial response is to "weathervane" into the wind. In a steady crosswind, the airplane will eventually stabilize with the wings approximately level and flying into the wind on a new heading. Basically, lateral wind shears do not cause large changes in altitude or airspeed. However, if large bank angles develop, a small loss of lift and rate of descent will be generated. Figure 4-8 shows the effect of a lateral sharp-edged gust having a 5 ft/sec intensity. Clearly, the horizontal

displacement is not very severe. The discrepancy between the longitudinal and the lateral responses is attributed to the different aerodynamic configurations seen by the wind.

Observing the lateral response due to air turbulence, one might conclude that lateral flight path corrections are not needed. However, it is known that deterministic models of lateral wind gusts can lead to unconservative results. Instead, one should refer to the random disturbance analysis. Stochastic results discussed in the previous chapter determined the need for both, lateral and vertical, trajectory corrections.
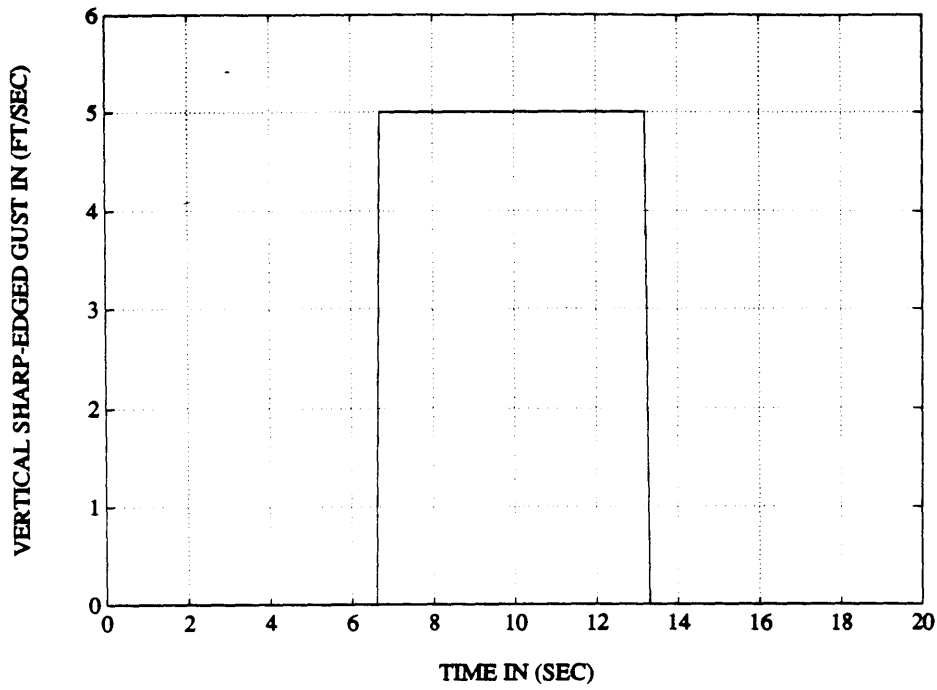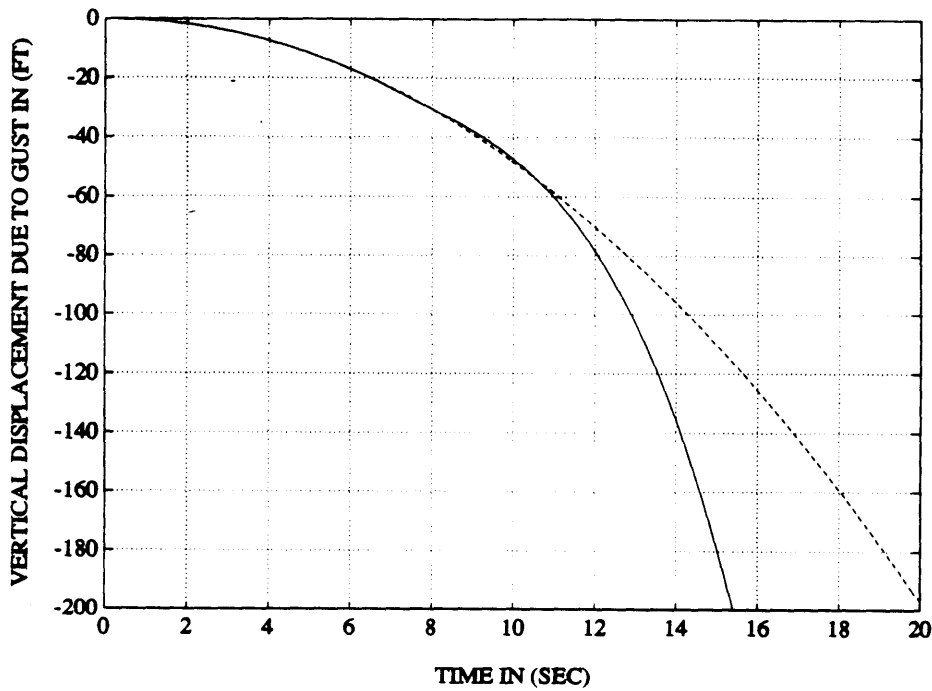
Figure 4-5: Simulated Vertical Sharp-Edged Gust

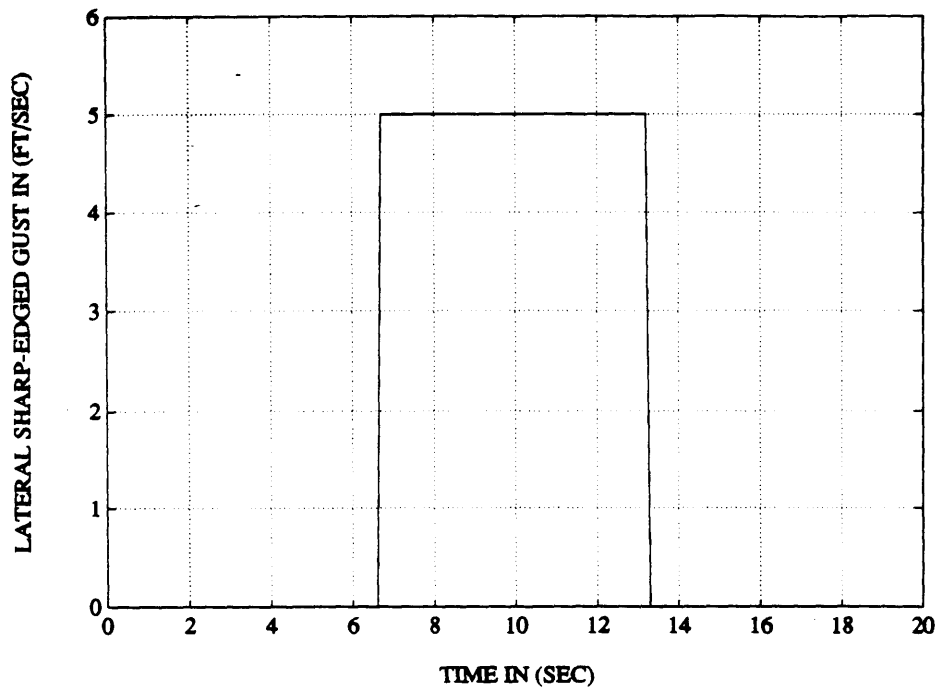Figure 4-6: Aircraft Trajectory Due to Vertical Gust

44

Figure 4-7: Simulated Lateral Sharp-Edged Gust

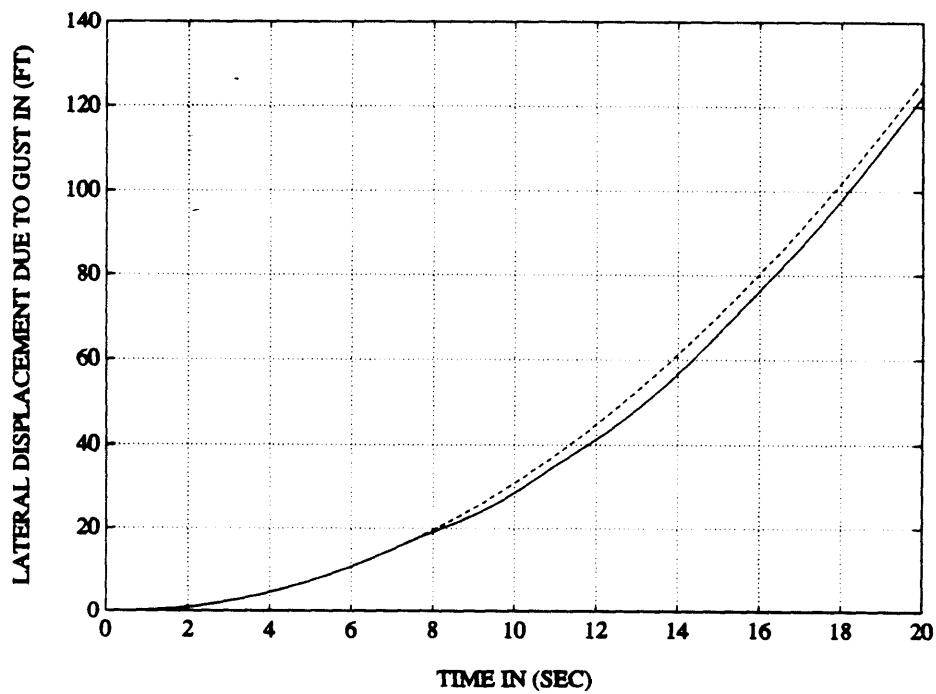Figure 4-8: Aircraft Trajectory due to Lateral Gust

Chapter 5

Complexity of Flight Control System Models

Results established in the two previous chapters dictate the necessity of continuous monitoring and control of the aircraft's position and velocity. Such monitoring is needed to closely track the commands generated by the planner in the presence of air turbulence. In addition, a radar altitude sensor and a forward-looking radar are unequivocally needed to avoid any imminent ground impact. This is necessary because of the expected low-altitude nature of the flight paths. The present chapter discusses how the flight commands are updated to compensate for trajectory deviations. The minimum degree of complexity of the flight control system models needed in the trajectory planner is also presented.

5.1   Command Updates

Since position and velocity feedbacks have been proved to be indispensable, the commands to the flight control systems must incorporate information about the flight path deviations. Between any set of two waypoints, the aircraft trajectory can be parametrized in time after implementing the appropriate commands. Consequently, an error vector, $\underline{e}$, described in the inertial coordinates system can be formed. It represents the deviation between the nominal and the actual trajectories at any instant.

The command updates consist of a linear combination of the components of the aircraft's position and velocity errors :

$$\tilde{a}_N = -K_1 e_z - K_2 \dot{e}_z \tag{5.1}$$

$$\tilde{\phi} = -K_3 e_y - K_4 \dot{e}_y \tag{5.2}$$

where the subscripts y and z designate respectively the lateral and vertical error components in the stability coordinates system. The reason for including the error rate, $\dot{\underline{e}}$, stems from the fact that it indicates future variations of the error vector, $\underline{e}$, and thus is helpful in stabilizing the loop. The gains, K_i, were selected by forming the equations describing the propagation of the state variable errors and using the linear quadratic approach. The objective was to minimize the magnitudes of the vectors $\underline{e}$ and $\dot{\underline{e}}$. The penalty matrices were chosen to make the gains that are not associated with the state variable errors $\underline{e}$ and $\dot{\underline{e}}$ vanishingly small. The resulting flight commands would then have the following form :

$$a_{Nc} = a_{Nn} + \tilde{a}_N \tag{5.3}$$

$$\phi_c = \phi_n + \tilde{\phi} \tag{5.4}$$

where a_{Nn} and ϕ_n are the nominal commands generated by the trajectory planner. Figures 5-3 and 5-5 show the aircraft's trajectory resulting from position and velocity feedbacks. It is assumed that the nominal commands are step functions and that a sharp-edged gust is present en route.

Comparing figures 5-3 and 5-5 to figures 4-6 and 4-8 where position and velocity feedbacks are absent, one can conclude that the command updates successfully resolved the problem of experiencing substantial deviations from the flight path that is predicted by the planner.

47

a_{Nc} → $\dfrac{1}{1+0.1s}$ → a_{Nr}
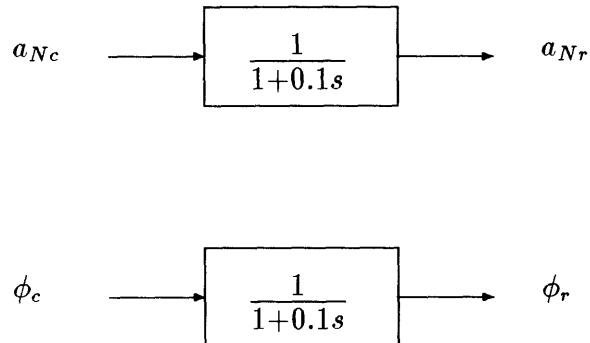
ϕ_c → $\dfrac{1}{1+0.1s}$ → ϕ_r

Figure 5-1: Simplified Models of Flight Control Systems

5.2   Model Simplification

Another important question remains to be addressed : How complex should the models of the flight control systems be in the optimization process ? This question was deferred to this point because it was anticipated that the answer would depend on whether or not continuous position and velocity feedbacks would be needed. To answer this question, two first order lags were used to model the flight control systems (see figure 5-1). The parameters of the simplified models were selected so that their step reponses would have the same settling time as the full dynamics models.

Although the order of the flight control systems has been dramatically reduced, it still remains to examine the corresponding trajectory. If flight path displacements caused by model simplification prove to be much larger than those caused by wind disturbances, the order of the control systems models will have to be augmented. Short period and Dutch roll approximations will have to be included in the design process. This would be in the direction of increasing the control systems complexity in order to keep modeling errors from exceeding the errors caused by air turbulence.

The validity of the models in figure 5-1 is determined by examining the trajectory deviations due to modeling errors. It is expected that modeling restrictions will be alleviated by requiring position and velocity feedbacks. This observation is based upon the sensitivity decrease of the aircraft's trajectory to modeling errors due to such feedbacks. Figures 5-6 and 5-7 show the vertical displacement errors generated by air turbulence and modeling errors respectively. Similar plots describing the horizontal displacement errors are presented in figures 5-8 and 5-9. Continuous feedbacks of position and velocity errors are used in each case.

It is obvious that errors resulting from simplified modeling are of the same order as those due to air turbulence. Therefore, it would be unnecessary to increase the complexity of the flight control systems for the purpose of achieving a more accurate trajectory following. As a concluding remark, it should be added that first order lags are the most simple representation into which models of flight control systems could be cast.
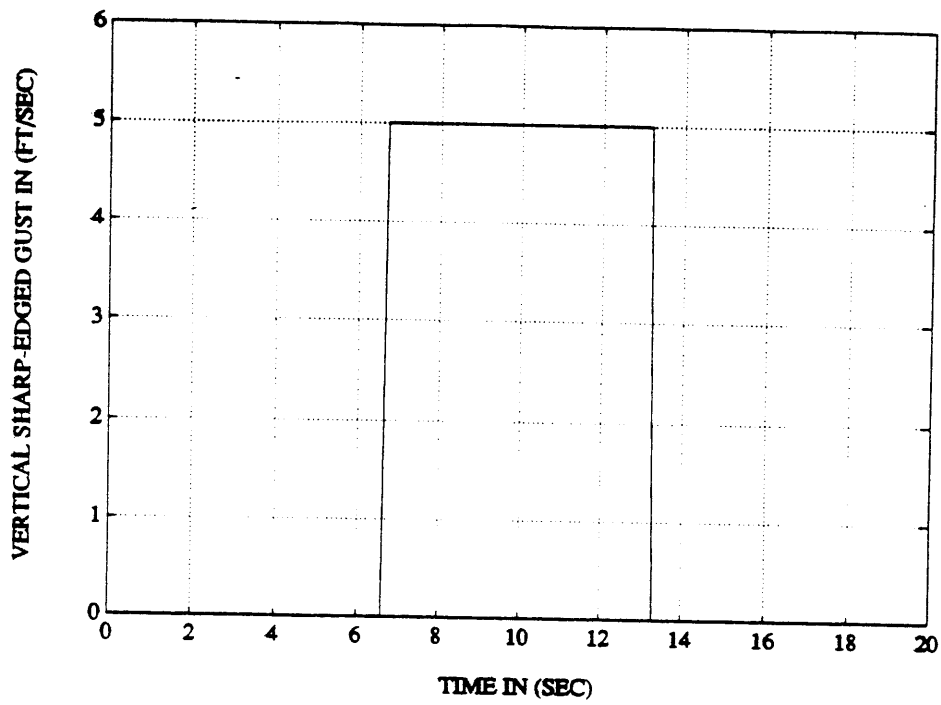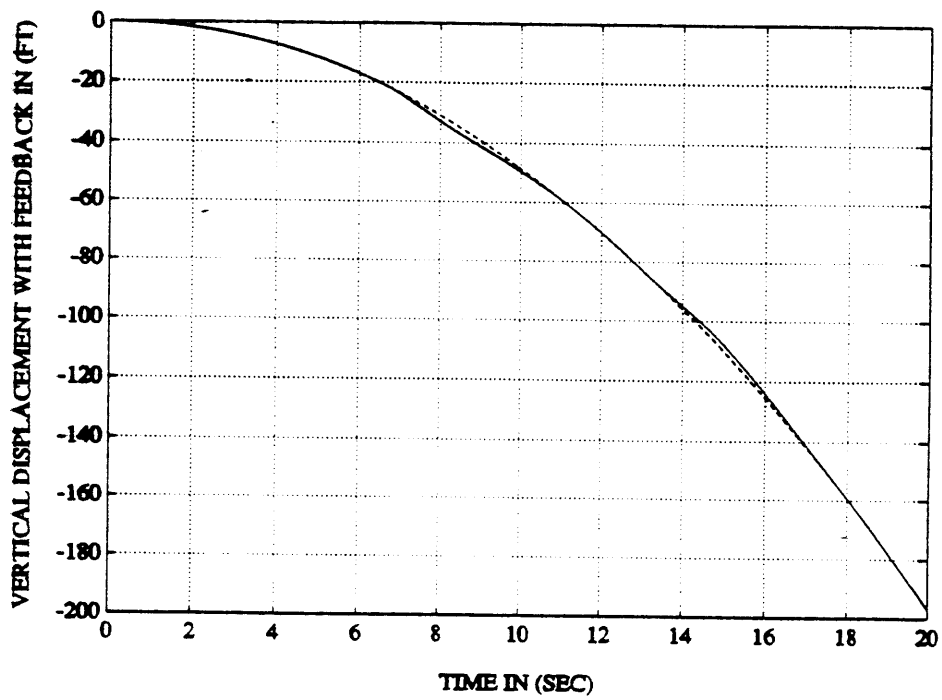
Figure 5-2: Vertical Sharp-Edged Gust

Figure 5-3: Aircraft Vertical Response with Position and Velocity Feedback
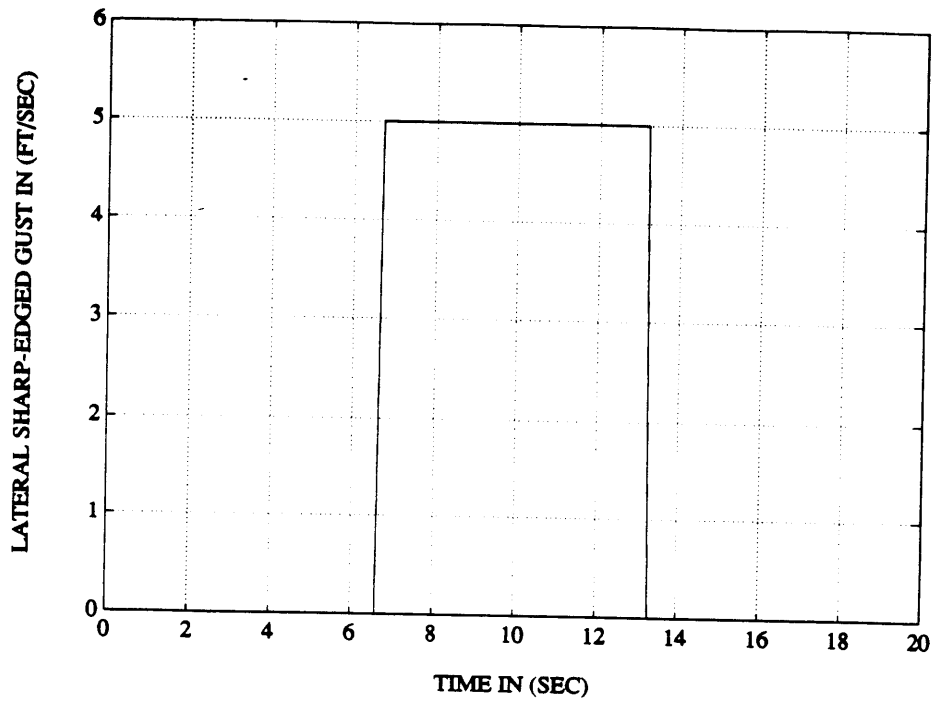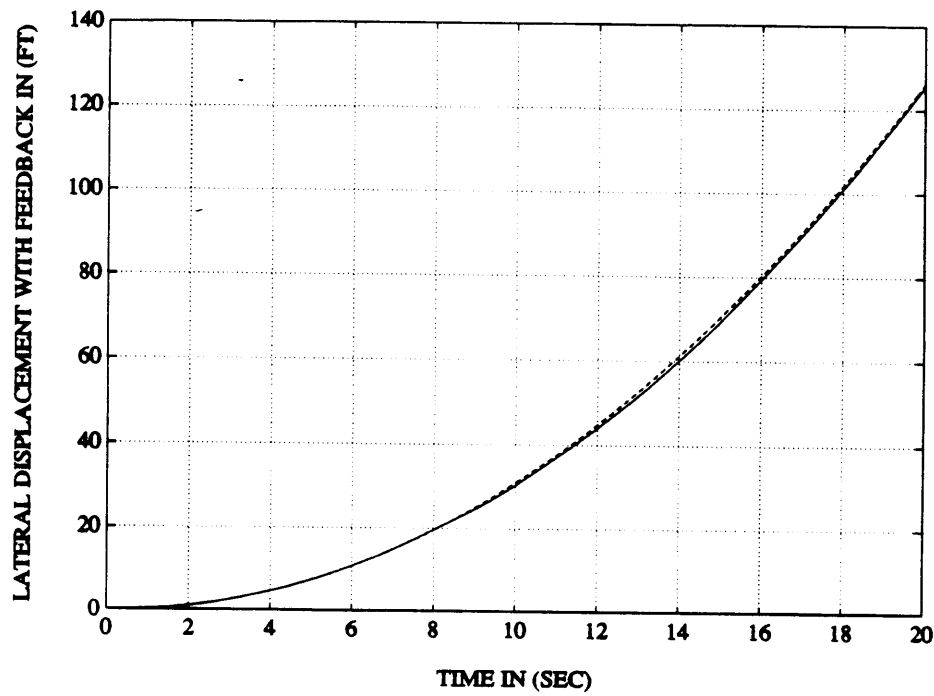
Figure 5-4: Lateral Sharp-Edged Gust

Figure 5-5: Aircraft Horizontal Response with Position and Velocity Feedbacks
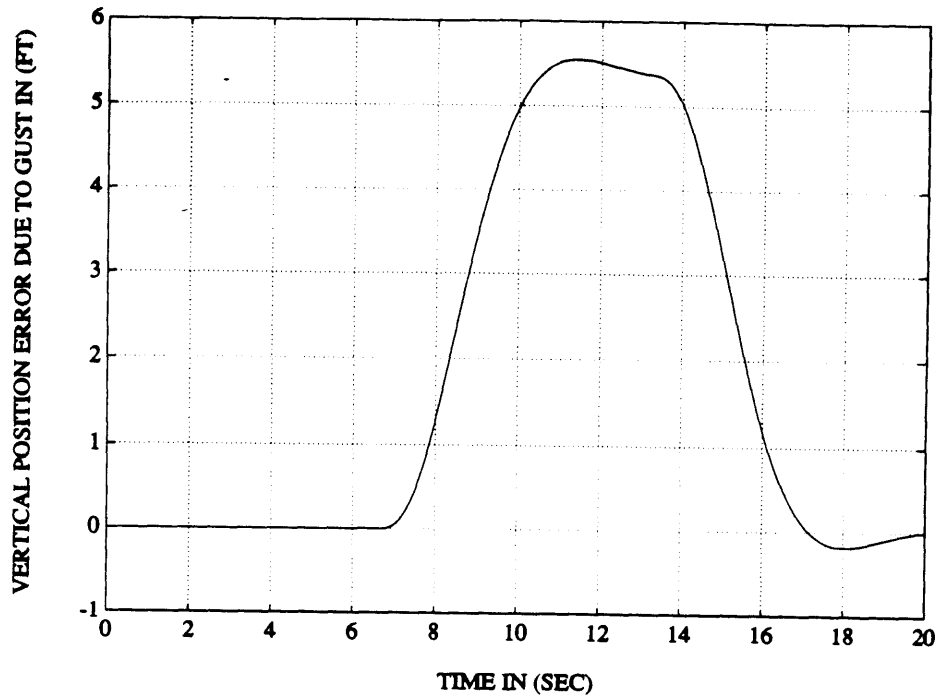
51

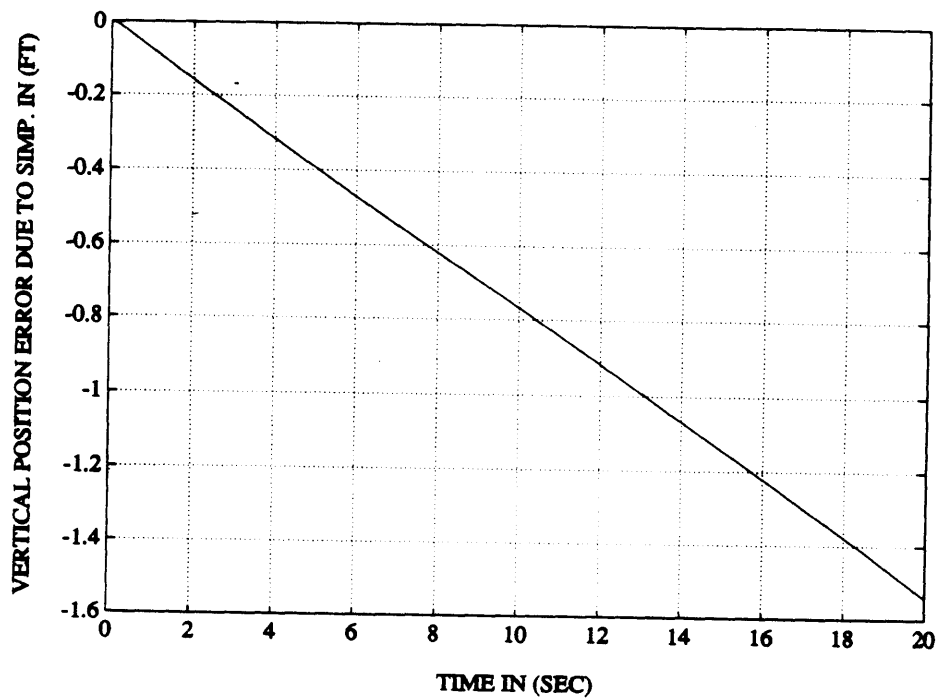Figure 5-6: Vertical Displacement Error Due to Wind Gust

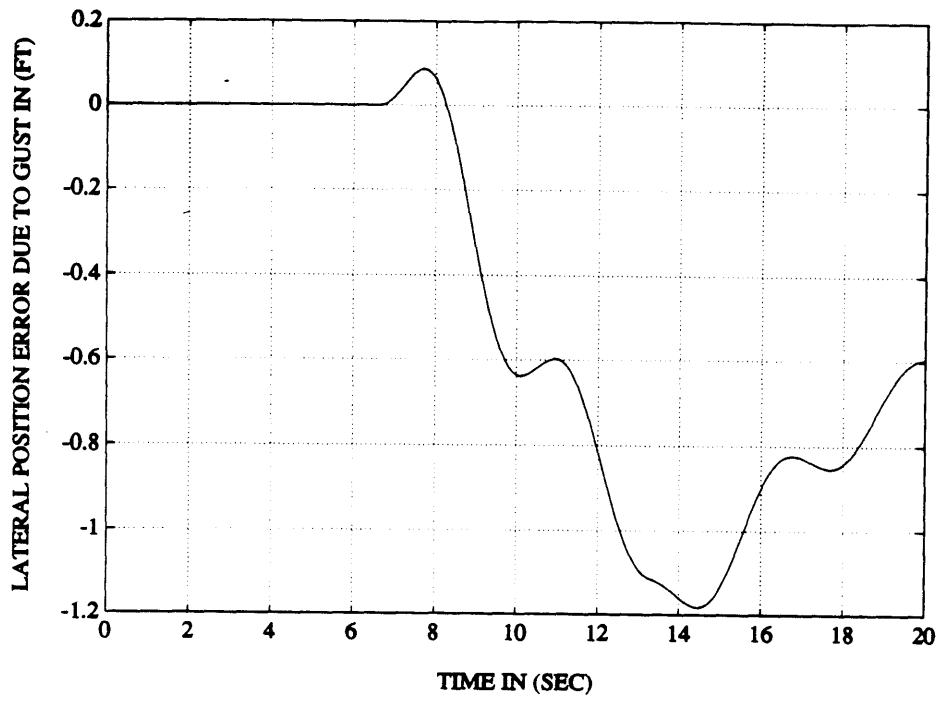Figure 5-7: Vertical Displacement Error Due to Modeling

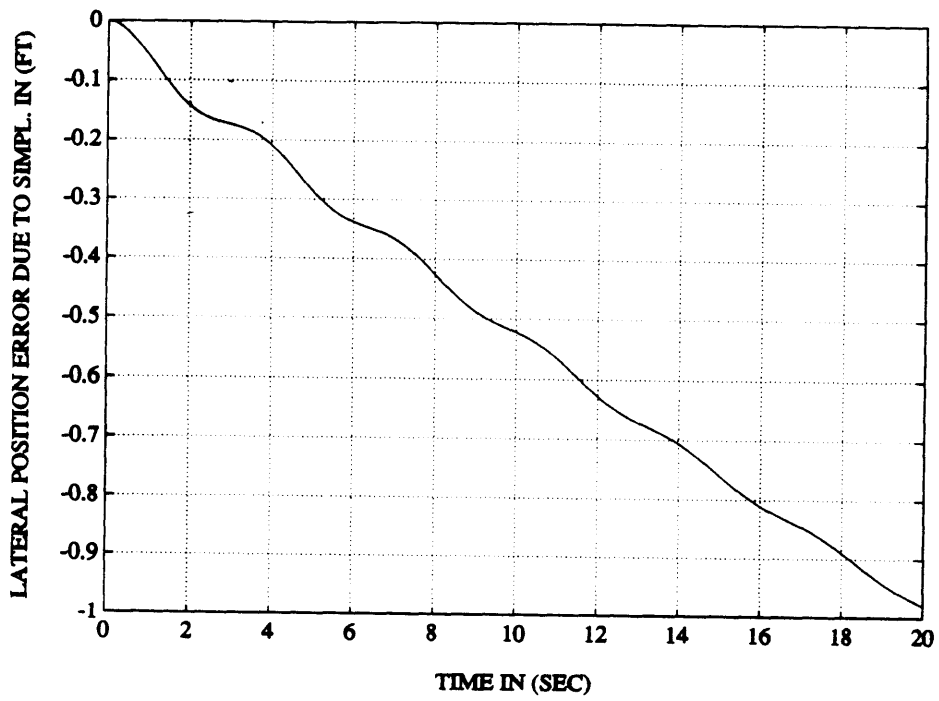Figure 5-8: Horizontal Displacement Error Due to Wind Gust

Figure 5-9: Horizontal Displacement Error Due to Modeling

53

Chapter 6

Conclusions and

Recommendations

6.1 Summary of Results

The minimum degree of complexity of the flight control systems models needed in the optimization process was determined in the context of position and velocity feedbacks. Since the aircraft is flying at very low altitudes, it was expected that position and velocity monitoring are needed to suppress the effects of wind disturbances. Stochastic and deterministic analyses of air turbulence were carried out and specific wind gust models were simulated.

Normal acceleration and bank angle command updates were used to minimize the sensitivity of the aircraft's trajectory against wind-induced deviations. The updates were based upon position and velocity errors between the actual flight path and the one predicted by the trajectory planner.

Once the computed trajectory was followed closely, even in the presence of wind gusts, simplified flight control systems models were developed. Use of the simplified models in the optimization process was justified by comparing trajectory deviations due to modeling errors to those that are due to air turbulence.

6.2 Further Research

Although it was possible to keep the complexity of the flight control systems models at a minimum, the issue of timely command generation remains to be investigated. This timeliness is directly associated with the mission success through avoidance of ground threats. Unless a powerful computer on board is used in the optimization process, a "back-up unit" must be available. The task of this unit would be to develop a reasonable strategy ensuring the safety of the mission until the optimal command history is available. It is expected that such strategy would account for terrain nature and the distribution of nearby threats. For instance, if the aircraft is flying over a flat terrain with widely dispersed ground threats, a sensible strategy might be to implement the most recent command history as the last waypoint is passed until convergence of the optimization algorithm is reached.

In this research, as well as in previous works [1, 2], it was assumed that the waypoints distribution is two dimensional. In reality, the waypoints generated by the goal point planner are depicted in three dimensions. A similar assumption applies to the threat database. A substantial work might be concentrated on a reliable command generation taking into account a three-dimensional threat database. Another direction for further research might be to simplify the optimization process. Reduced computational tasks translate into rapid convergence and, consequently, relieving the need for a "back-up unit".

Finally, it would be interesting to implement the concept of the mission planning system in real-time. Using simplified models of the flight control systems, the aircraft response to the generated commands should be evaluated via comparing the actual flight path to the one predicted by the trajectory planner.

Bibliography

[1] Alexander, J.R., *Aircraft Command Interface for a Real-Time Trajectory Planning System*, Master's Thesis, Massachusetts Institute of Technology, 1988.

[2] Walker, W.J., *Flight Control Command Generation in a Real-Time Mission Planning System*, Master's Thesis, Massachusetts Institute of Technology, 1990.

[3] Etkin, B., *Dynamics of Flight*, Wiley, New York, 1959.

[4] Hoblit, F.M., *Gust Loads on Aircraft : Concepts and Applications*, AIAA Press, Washington, DC, 1988.

[5] Freudenberg, J.S., and D.P. Looze, *Frequency Domain Properties of Scalar and Multivariable Feedback Systems*, Springer-Verlag, 1988.

[6] Boyd, S. and Desoer, C.A., *Subharmonic Functions and Performance Bounds on Linear Time-Invariant Feedback Systems*, IMA Jour. of Infor. and Contr., 1985.

[7] McRuer, D., I. Ashkenas, and D. Graham, *Aircraft Dynamics and Automatic Control*, Princeton University Press, Princeton, NJ, 1973.

[8] Nelson, R.C., *Flight Stability and Automatic Control*, McGraw-Hill, New York, 1989.